

RESEARCH PAPER



Discovery of new quinolines as potent colchicine binding site inhibitors: design, synthesis, docking studies, and anti-proliferative evaluation

Mohamed Hagra^a, Moshira A. El Deeb^b, Heba S. A. Elzahabi^c, Eslam B. Elkaeed^{d,a}, Ahmed B. M. Mehany^e and Ibrahim H. Eissa^f

^aDepartment of Pharmaceutical Organic Chemistry, Faculty of Pharmacy (Boys), Al-Azhar University, Cairo, Egypt; ^bDepartment of Pharmaceutical Organic Chemistry, Faculty of Pharmacy (Girls), Al-Azhar University, Cairo, Egypt; ^cDepartment of Pharmaceutical Medicinal Chemistry & Drug Design, Faculty of Pharmacy (Girls), Al-Azhar University, Cairo, Egypt; ^dDepartment of Pharmaceutical Sciences, College of Pharmacy, AlMaarefa University, Ad Diriyah, Riyadh, Saudi Arabia; ^eDepartment of Zoology, Faculty of Science, Al-Azhar University, Cairo, Egypt; ^fDepartment of Pharmaceutical Medicinal Chemistry & Drug Design, Faculty of Pharmacy (Boys), Al-Azhar University, Cairo, Egypt

ABSTRACT

Discovering of new anticancer agents with potential activity against tubulin polymerisation is still a promising approach. Colchicine binding site inhibitors are the most relevant anti-tubulin polymerisation agents. Thus, new quinoline derivatives have been designed and synthesised to possess the same essential pharmacophoric features of colchicine binding site inhibitors. The synthesised compounds were tested *in vitro* against a panel of three human cancer cell lines (HepG-2, HCT-116, and MCF-7) using colchicine as a positive control. Comparing to colchicine (IC_{50} = 7.40, 9.32, and 10.41 μ M against HepG-2, HCT-116, and MCF-7, respectively), compounds **20**, **21**, **22**, **23**, **24**, **25**, **26**, and **28** exhibited superior cytotoxic activities with IC_{50} values ranging from 1.78 to 9.19 μ M. In order to sightsee the proposed mechanism of anti-proliferative activity, the most active members were further evaluated *in vitro* for their inhibitory activities against tubulin polymerisation. Compounds **21** and **32** exhibited the highest tubulin polymerisation inhibitory effect with IC_{50} values of 9.11 and 10.5 nM, respectively. Such members showed activities higher than that of colchicine (IC_{50} = 10.6 nM) and CA-4 (IC_{50} = 13.2 nM). The impact of the most promising compound **25** on cell cycle distribution was assessed. The results revealed that compound **25** can arrest the cell cycle at G2/M phase. Annexin V and PI double staining assay was carried out to explore the apoptotic effect of the synthesised compounds. Compound **25** induced apoptotic effect on HepG-2 thirteen times more than the control cells. To examine the binding pattern of the target compounds against the tubulin heterodimers active site, molecular docking studies were carried out.

ARTICLE HISTORY

Received 6 December 2020
Revised 26 December 2020
Accepted 25 January 2021

KEYWORDS

Cancer; colchicine binding site inhibitors; docking; quinoline; tubulin polymerisation

1. Introduction

Cancer is the uncontrolled growth of abnormal cells¹. There are about 100 types of cancer which need diagnosis and treatment². In 2018, according to National Cancer Institute (NIH), approximately 1,735,350 new cases of cancer have been diagnosed in the United States and 609,640 people died from the disease. Cancer of breast, liver, colon, and rectum are common disease with high rate of incidence³. The current approaches of cancer treatment include surgery, radiation, chemotherapy; and hormonal treatment⁴.


Microtubules are important cytoskeletal structures that have a crucial role in cell division⁵, which make them attractive targets for design of new anticancer agents^{6,7}. Microtubules are composed of two subunits of α - and β -tubulin heterodimers. These subunits are arranged in slender-shaped filamentous tubes with many micrometres long⁸. Some natural products that target the tubulin and the microtubule system- also referred to as

anti-mitotics-still important counterparts in combination chemotherapy for the treatment of several malignancies^{9,10}.

The tubulin heterodimer comprises at least three binding sites: the paclitaxel, vinblastine, and colchicine binding sites (Figure 1)¹¹. There are many drugs used in clinical oncology acting on the paclitaxel and vinblastine binding sites^{12,13}. These drugs are highly potent but there are some limitation in clinical use for many reasons: development of multi-drug resistance, high lipophilicity, low water solubility, intravenous administration due to poor water solubility¹⁴. Aforementioned drawbacks can largely overcome by use of tubulin inhibitors that bind to the colchicine binding site. Such inhibitors have therapeutic advantages: high water solubility so that it can be administered orally and there is no multi-drug resistance¹⁵.

Colchicine binding site inhibitors (CBSI) produce their biological activities by suppressing the vital process of tubulin assembly, and consequently suppressing microtubule formation¹⁴. Colchicine I, the most famous inhibitors in this category, binds to tubulin very tightly, but there is no any compound in this group has a

CONTACT Ibrahim H. Eissa  ibrahimeissa@azhar.edu.eg  Department of Pharmaceutical Medicinal Chemistry & Drug Design, Faculty of Pharmacy (Boys), Al-Azhar University, Cairo 11884, Egypt; Mohamed Hagra  m.hagrs@azhar.edu.eg  Department of Pharmaceutical Organic Chemistry, Faculty of Pharmacy (Boys), Al-Azhar University, Cairo 11884, Egypt

 Supplemental data for this article can be accessed [here](#).

© 2021 The Author(s). Published by Informa UK Limited, trading as Taylor & Francis Group.

This is an Open Access article distributed under the terms of the Creative Commons Attribution License (<http://creativecommons.org/licenses/by/4.0/>), which permits unrestricted use, distribution, and reproduction in any medium, provided the original work is properly cited.



Figure 1. Reported colchicine binding site inhibitors.

significant use in treatment of cancer¹⁶. combretastatin A-1 (CA-1) **II** and combretastatin A- 4 (CA-4) **III** are combretastatin analogs having microtubule inhibitory activity with limited value due to their low water solubility¹⁷. To improve their water solubility, such analogs were designed as prodrugs of monosodium phosphate salt. These prodrugs can be metabolised *in vivo* into CA-1 and CA-4 as active components^{18,19}. CA-4P showed no bone marrow toxicity, stomatitis, and hair loss in phase II clinical trial²⁰. One of CA-4 analogs is omrabulin **IV** which has better water solubility, oral activity, enhanced anti-cancer activity and decreased adverse effects¹⁴.

Plinabulin **V** is an active molecule against non-small cell lung cancer²¹. It restricts tubulin polymerisation with immune-enhancing effects^{22,23}. Indibulin **VI** has an effective antitumor activity

with a lower side effects²⁴. The antitumor activity of indibulin is believed to be related to its effects on microtubules²⁵.

E7010 **VII** is an orally bioavailable tubulin-binding agent that was developed for cancer treatment. It is a sulphonamide derivatives having an antimitotic effect. It binds to the colchicine site on β -tubulin subunit, leading to cell cycle arrest at the G2/M phase, resulting in cellular apoptosis²⁶. It exhibited a broad spectrum of antitumor activity *in vitro* and *in vivo*²⁶. Its clinical trial indicated that it has dose-limiting toxicities included abdominal pain, constipation, and fatigue¹⁴.

Podophyllotoxin **VIII**, a naturally occurring anticancer agent, binds to the colchicine site of tubulin leading to inhibition of the tubulin assembly into microtubules²⁷. It has severe toxicity which limits its clinical application as a cancer therapy. However,

podophyllotoxin is still considered an attractive lead compound for the generation of new antitumor agents²⁸.

Moreover, several derivatives (e.g. compounds **IX**²⁹, **X**³⁰, **XI**³¹, and **XII**³²) has been synthesised and evaluated as tubulin inhibitors targeting the colchicine binding site. These compounds were modified and tested to find highly potent agents for treatment of cancer.

In continuation to our previous efforts of design and synthesis of new anticancer agents^{33–42}, a new series of quinoline derivatives were designed and synthesised. The synthesised derivatives have the same pharmacophoric features of CBSI to examine their effect as anticancer agents with potential tubulin inhibitory activities targeting the colchicine binding site.

1.1. Rational of molecular design

The colchicine binding site is a funnel shaped with a volume of about 600 Å. the cavity of the active site is surrounded by Ala180 α , Asn101 α , Thr179 α , Val181 α , Thr314 β , Asn349 β , Lys352 β , Asn350 β , Tyr202 β , Thr239 β , Asp251 β , Cys241 β , Asn258 β , Leu242 β , Leu248 β , Leu252 β , Ile378 β , Leu255 β , Val318 β , Ala250 β , Lys254 β ,

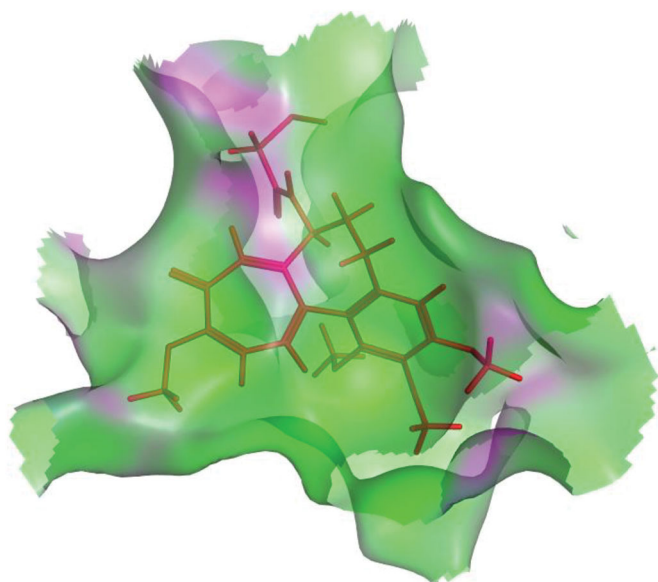


Figure 2. The colchicine binding site having a funnel shape.³⁹

Ala316 β , Met259 β , Ala317 β , Val238 β , Thr353 β , and Ala354 β residues (Figure 2)^{39,43}.

It was reported that the colchicine binding site inhibitors possess seven essential pharmacophoric groups; one hydrogen bond donor (D1), three hydrogen bond acceptors (A1, A2, and A3), two hydrophobic centres (H1 and H2), and one planar group (R1)^{14,44} (Figure 3(A)). The different pharmacophoric features are arranged in two planes. The Features A1, D1, H1, and R1 lie in plane A, and features A2, A3, and H2 lie in plane B. The angle between the two planes is about 45°^{39,44} (Figure 3(B)).

Colchicine as a prototype of CBSIs is formed of three rings (A, B linker), and C). some reports revealed that A- and C-ring encompasses the least pharmacophoric features required for binding to tubulin⁴⁵. In addition, it was found that changes in the ring B (linker) could affect the antiproliferative activity the CBSIs³¹. Figure 4 shows the pharmacophoric points on colchicine and podophyllotoxin as representative examples of CBSIs.

The main target of this work was the synthesis of new quinoline derivatives having the same essential pharmacophoric features of the reported CBSIs (Figure 5). The core of our molecular design rational comprised bioisosteric modification strategies of CBSIs at three different positions (Figure 6).

The first position was the C-ring, where the 2-chloro-6-methoxyquinoline moiety used as a bioisosteric ring equivalent. The second position was the B-ring (linker region), where different hetero-rings were used including five-membered rings as 4,5-dihydro-1H-pyrazole (compounds **8–10** and **14–25**) and 4,5-dihydroisoxazol (compounds **11–13**), or six-membered rings as pyrimidine-2(1H)-thione (compounds **26–28**), 2-aminopyrimidine (compounds **29–31**), and pyrimidin-2(1H)-one (compounds **32–34**). The third position was the A-ring, where different substituted phenyl rings were used including 4-chlorophenyl, 4-amino-phenyl, and 3,4,5-trimethoxyphenyl.

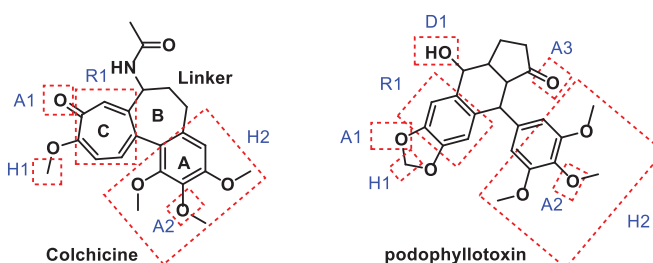


Figure 4. Pharmacophoric points of colchicine and podophyllotoxin as CBSIs.

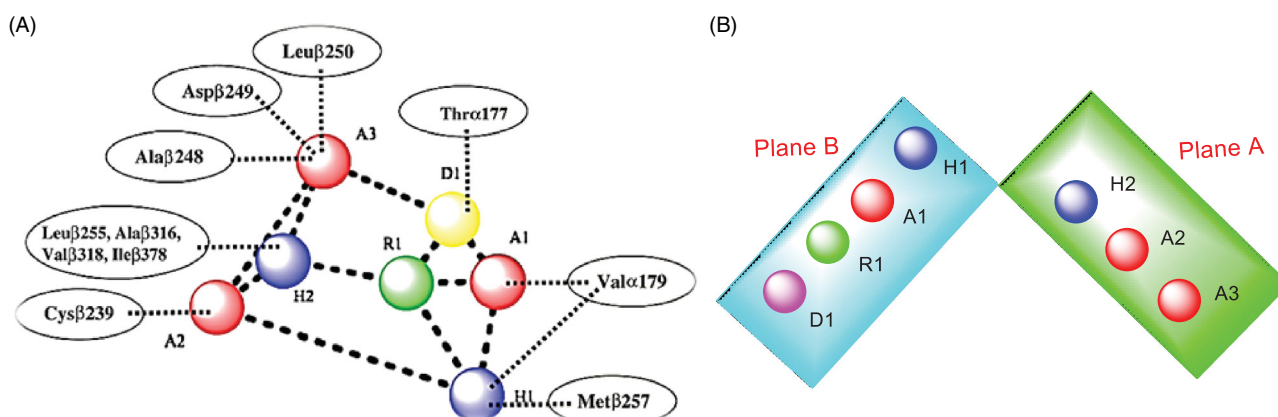


Figure 3. (A) Seven pharmacophoric features of colchicine binding site inhibitors: three hydrogen bond acceptors (A1, A2 & A3), one hydrogen bond donor (D1), two hydrophobic centres (H1 & H2), and one planar group (R1) (based on Ref.^{14,44}). (B) The pharmacophoric model with two planes: plane A (green) points A1, D1, H1 and R1, Plane B (turquoise) consists of points A2, A3, and H2, and (based on Ref.^{39,44}).

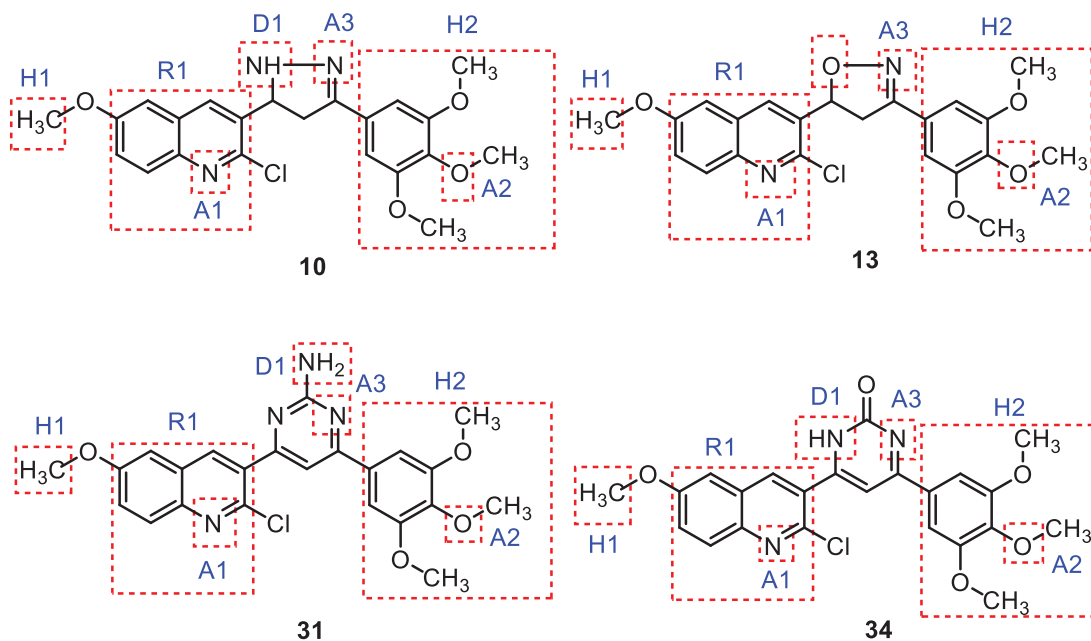


Figure 5. Representative examples of the newly synthesised compounds having the same essential pharmacophoric features of the CBSIs.

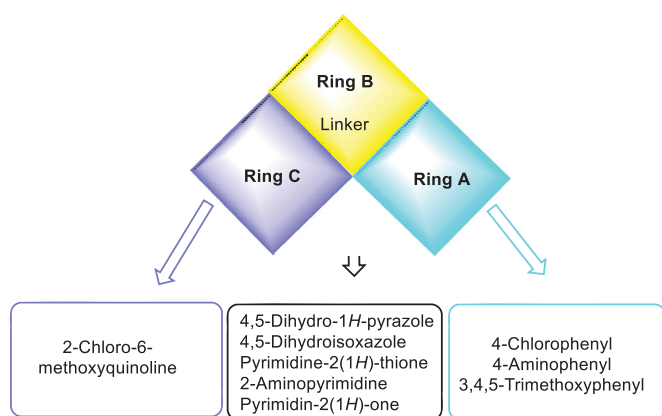


Figure 6. Summary for all chemical modifications.

The wide variety of modifications enabled us to study the SAR of these compounds as effective anti-cancer agents with potential tubulin inhibitory activity which is considered as a crucial objective of our work. All modification pathways and molecular design rationale were illustrated and summarised in Figure 7.

2. Results and discussion

2.1. Chemistry

The synthetic pathways employed to prepare the target compounds are outlined in Schemes 1–3. Firstly, *p*-aminoacetophenone **1** was refluxed in acetic anhydride/sodium acetate mixture to produce *N*-(4-methoxyphenyl) acetamide **2**. Boiling compound **2** with POCl_3 in the presence of catalytic amount of DMF, produced aldehyde derivative **3**. Chalcone derivatives **5**, **6**, and **7** were prepared through the reaction of compound **3** with the corresponding acetophenones **4** in the presence of alcoholic NaOH. The reaction occurred by ratio (1:1) to form chalcone which crystallised from ethanol, the structure of compounds **5**, **6**, and **7** were established on the basis of its elemental and spectral data. The IR spectra of compounds **5**, **6**, and **7** were characterised by

strong absorption bands around 1655 cm^{-1} due to carbonyl ketone stretching, which appeared at low absorption value because of extended conjugation with the double bond. The absolute geometry of the α,β -unsaturated carbonyl linker was assigned to be in *trans* form based on the coupling constant alkene protons. In more details, the ^1H NMR spectrum of chalcone **5** showed two doublets, each equivalent to one proton, at δ 8.1 ppm due to CH alkene (β -proton) and at δ 7.9 ppm due to CH alkene (α -proton). Both protons have the same coupling constant value of 15.2 Hz, which confirms the *E*-configuration. Additionally, the ^1H NMR spectrum of compound **5** displayed two more doublets, each of two protons, at δ 8.2 and 7.1 ppm, with coupling constant value of 8.4 Hz which is attributed to the *p*-disubstituted phenyl moiety (Scheme 1, Supplementary data).

The reactivity of chalcone can be attributed to the fact that their molecules have two electron poor centres at C-1 and C-3 in addition to one electron rich centre at C-2, so the double bond in chalcone can be looked on as an electron rich bond that may enter in 1,3-dipolar cycloaddition reactions. Chalcone are heavily utilised synthons in 1,3-cycloaddition reactions to build a wide variety of heterocyclic systems such as pyrrolidines, oxazolines and pyrimidines. In this work, nine different 1,3-dipolar cyclo-addition reactions have been achieved. All reactions proceeded smoothly and final products were obtained in relatively good yields as detailed in the experimental part. The subsequent paragraphs point out those reactions in depth (Scheme 2).

First, to build a dihydropyrazole ring system, a mixture of the chalcone (**5**, **6**, and **7**) with excess hydrazine hydrate in absolute ethanol was heated up at reflux temperature to finally give the desired corresponding compounds **8**, **9**, and **10**. The structure of compound **8** was established on the basis of its elemental and spectral data. IR spectrum of compound **8** exhibited an important band at 3295 cm^{-1} due to NH stretching of the newly formed dihydropyrazole ring. The later NH was also appeared on the ^1H NMR spectrum as a broad deuterium-exchangeable singlet within the aromatic region at δ 7.1 ppm. The hydrocarbon backbone of the newly built dihydropyrazole ring revealed three more signals; i.e. a triplet, of one proton at δ 5.1 ppm due to pyrazole-H5 that

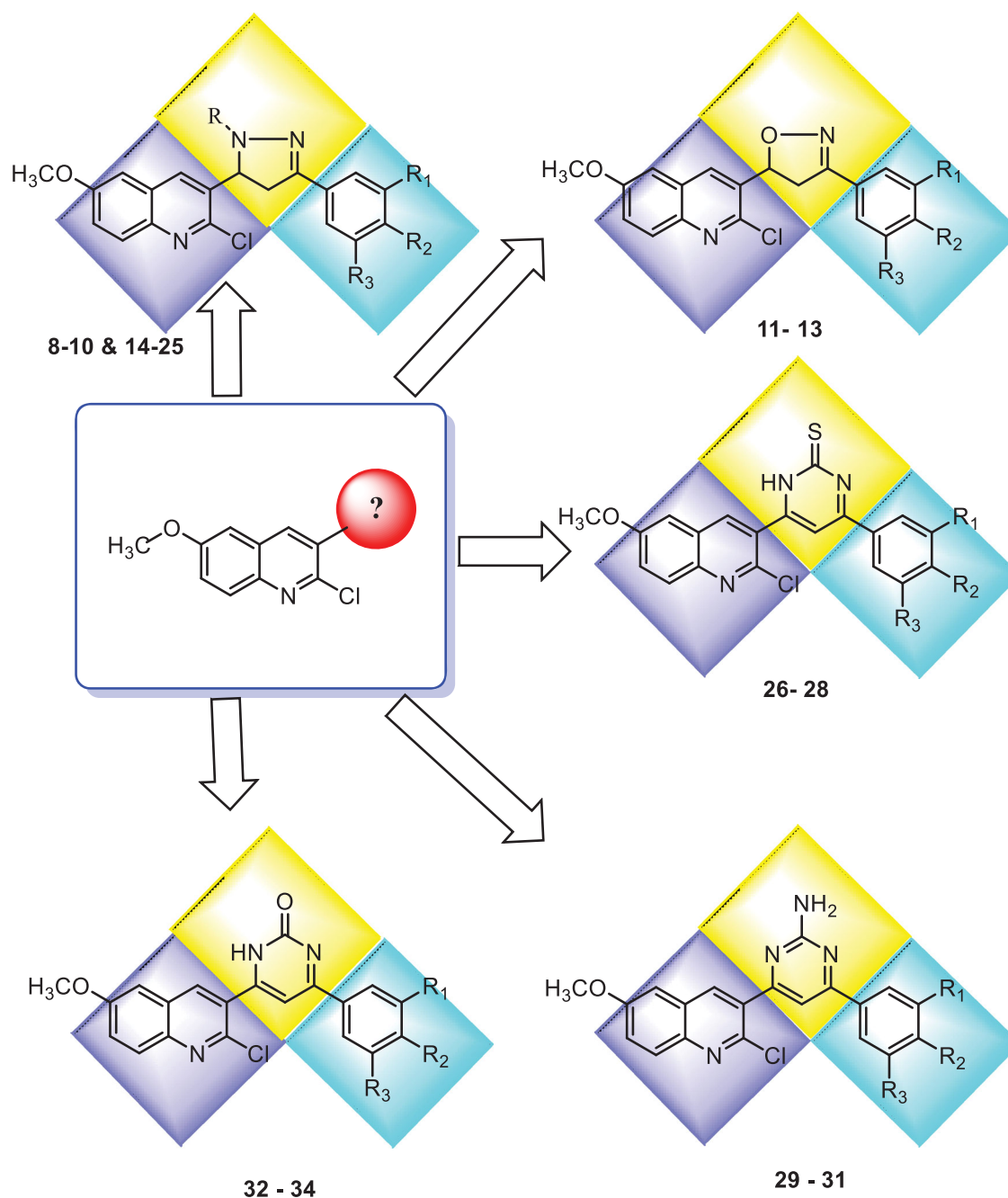


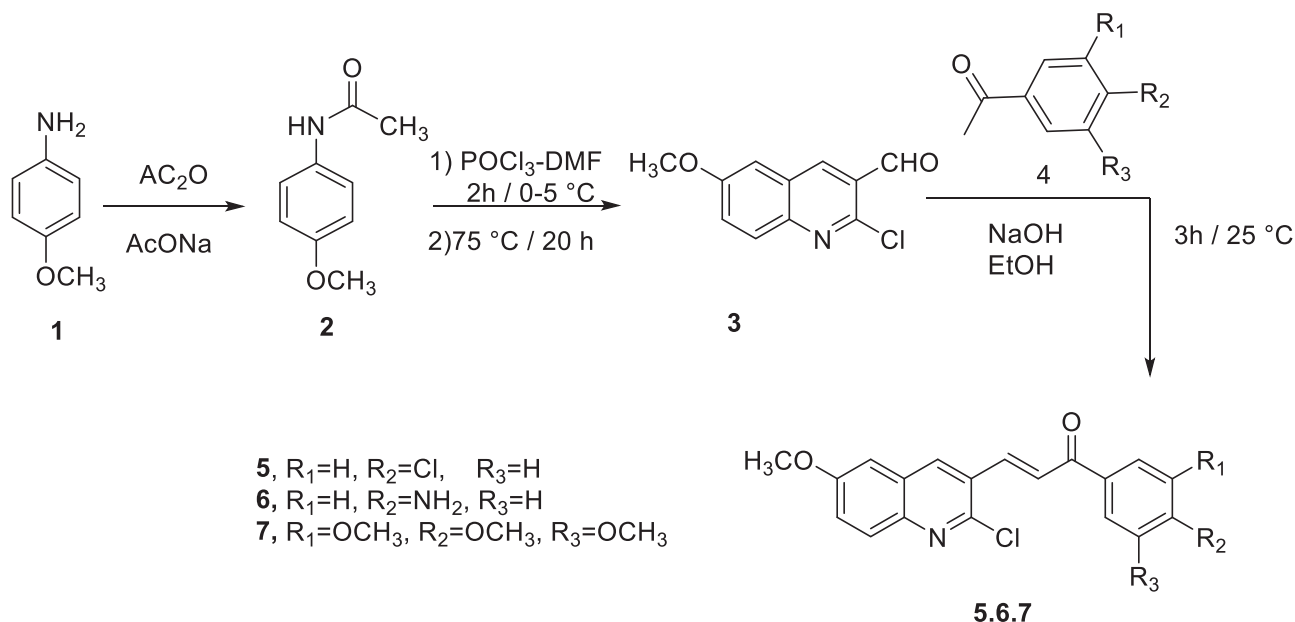
Figure 7. Rational of molecular design of the new proposed CBSIs.

appeared downfield, as expected, because of the neighbouring nitrogen atom; on the other hand, there were two doublet of doublets, each of one proton at δ 3.7 and 2.8 ppm with coupling constants of 5.6 and 16.8 Hz assignable for pyrazole-H4 axial proton, 9.6 and 16.4 Hz of pyrazole-H4 equatorial proton. In addition, mass spectrum of compound **8** showed a strong base peak with the proper chlorine-isotope distribution pattern (see experimental part). Formation of dihydropyrazole derivatives were postulated to pass through two steps. The first step involves Michael-type addition on carbonyl β -carbon, followed by protonation to afford β -hydrazinylpropanone intermediate. The terminal primary amine attacks the carbonyl group to finally give the dihydropyrazole final product after loss a molecule of water as detailed below (Supplementary data).

Next, to synthesise dihydroisoxazole derivatives **11**, **12**, and **13**, a mixture of chalcone (**5,6,7**), hydroxylamine hydrochloride,

and NaOH in ethanol was heated up till reflux to give the corresponding target compounds **11**, **12**, and **13**. The IR spectra of compound **11** characterised by a band at 1590 cm^{-1} due to C=N, ^1H NMR spectra of compound **11** showed, a doublet of doublet of one proton at δ 6 ppm due to isoxazole-H5 which appeared downfield as expected because C-5 of isoxazole attached to oxygen atom, a two doublet of doublet, each equivalent for one proton at δ 4.0 and 3.5 ppm which attributed to isoxazole-H4 axial proton and isoxazole-H4 equatorial proton with coupling constant (11.2, 16.8 Hz) of axial proton and (6.8, 17.2 Hz) of equatorial proton, respectively, the most characteristic feature of ^1H NMR spectrum of compound **11** is the disappearance of the olefinic protons (Supplementary data).

Next, to prepare pyrimidine-2(1H)-thione derivatives **26,27**, and **28**, a mixture of chalcone, thiourea, and NaOH in ethanol was heated to reflux to give the corresponding target derivatives.



Scheme 1. Synthesis of the target compounds 5–7.

Taking compound **26** as an example, the IR spectrum was characterised by a band at 3308 cm^{-1} assignable to one NH stretching, the ^1H NMR spectrum shows, a singlet of one proton at 14.1 ppm due to NH which is D_2O exchangeable, a singlet for one proton at δ 8.6 ppm due to quinoline-H4, a doublet for one proton at δ 8.3 ppm due to quinoline-H8 with coupling constant 8.8 Hz, a doublet of two protons at δ 8.1 ppm due to phenyl-H2,H6 with coupling constant 8.4 Hz, a doublet for one proton at 7.8 ppm due to quinoline-H7 with coupling constant 8.8 Hz, a doublet of two protons at δ 7.5 ppm due to phenyl-H3,H5 with coupling constant 8.4 Hz, a singlet for one proton at 7.4 ppm due pyrimidine-H5, a singlet of one proton at δ 7.3 ppm due to quinoline-H5, a singlet of three protons at δ 3.8 ppm due to OCH_3 of quinoline (Scheme 3).

Similarly, pyrimidin-2-amine was synthesised. Briefly, a mixture of chalcone, guanidine hydrochloride, and NaOH in ethanol was heated to reflux to give the corresponding compounds **29**, **30**, and **31**. The structure of the isolated product was confirmed by spectral data, taking compound **29** as a representative example, the IR spectrum characterised by a band at 3320 and 3284 cm^{-1} due to NH_2 stretching, the ^1H NMR spectrum revealed a singlet for one proton at δ 8.4 ppm due to quinoline-H4, a doublet of one proton at δ 8.3 ppm due to quinoline-H8 with coupling constant 8.8 Hz, a doublet for two protons at δ 7.9 ppm due to phenyl-H2,H6 with coupling constant 8.4 Hz, a singlet of one proton at δ 7.5 ppm due to pyrimidine-H5, a singlet of one proton at 7.1 ppm due to quinoline-H5, a doublet of two protons at 7 ppm due to phenyl-H3,H5, a doublet for one proton at δ 6.7 ppm due to quinoline-H7 with coupling constant 8.8 Hz, a singlet for two protons at 5.4 ppm which attributed to NH_2 , D_2O exchangeable, a singlet of three protons at 3.7 ppm due to OCH_3 of quinoline.

Unlike other reactions in this series, reaction of chalcone with urea was preceded first under basic conditions, but the yield was poor, therefore we shifted towards the acidic medium. In brief, compounds **32**, **33**, and **34** were prepared, in a good yield, by allowing the corresponding chalcone to react with urea in the presence of conc. hydrochloric acid at a reflux temperature. Under strong acidic media, an alternative product was also anticipated, where the chlorine atom was expected to be hydrolysed to afford the amide-containing structure. Later structure was excluded

mainly base on the absence its molecular ion peak from the MS. Other spectral and elemental data confirm this assumption and confirm the structure of compounds **32**, **33**, and **34** (Supplementary data).

2.2. Biological evaluation

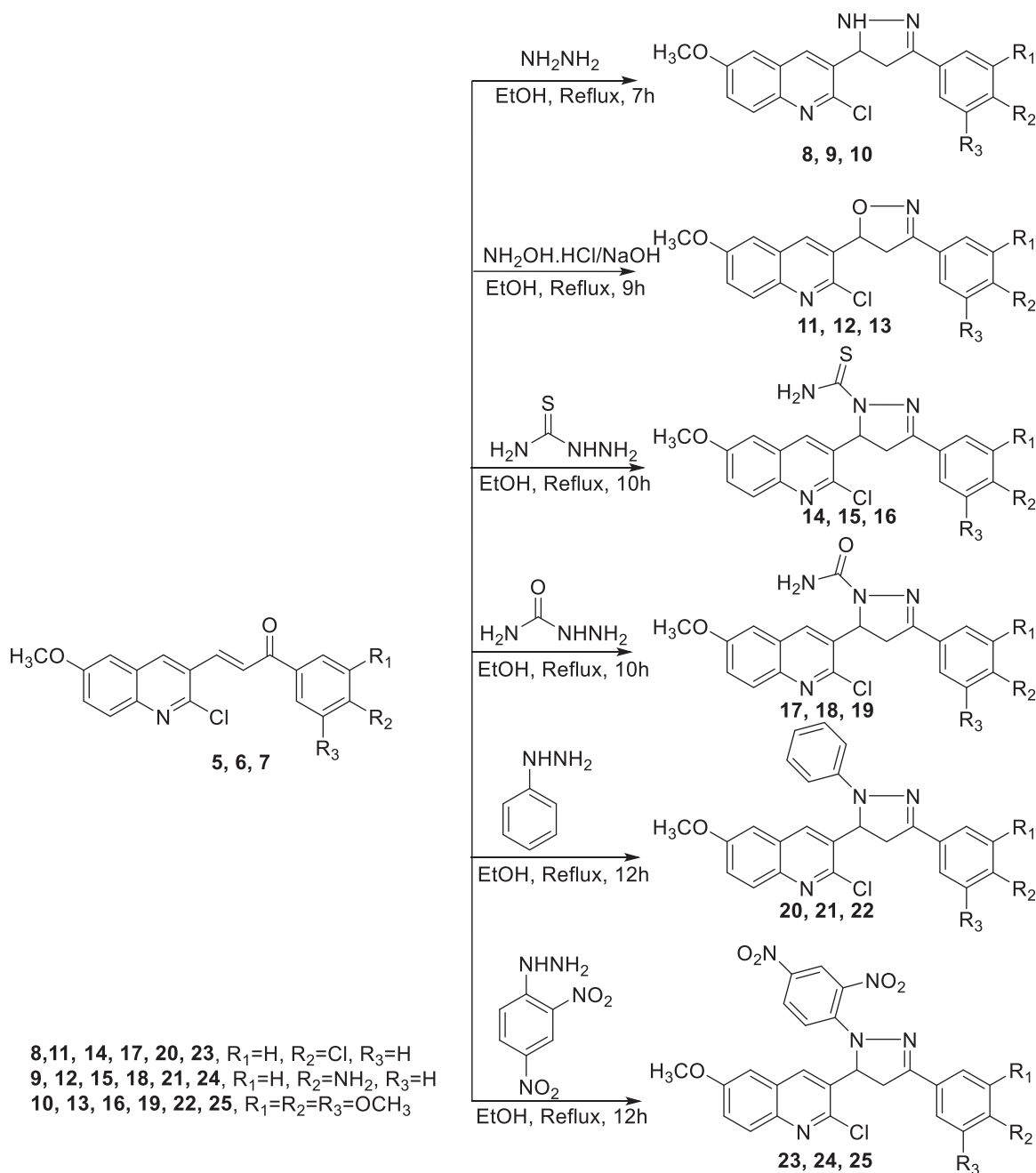
2.2.1. In vitro anti-proliferative activity

In vitro cytotoxic activities of the synthesised compounds were assessed using standard MTT method^{46–48}. a panel of human cancer cell lines namely; hepatocellular carcinoma (HepG-2), colorectal carcinoma (HCT-116), and breast cancer (MCF-7) were used in this test utilising colchicine as a reference standard. The antiproliferative activity was expressed in IC_{50} values as reported in Table 1.

From the cytotoxic screening, the tested compounds showed different degrees of activities against the tested cells. In general, some compounds were proven to be efficient anticancer candidates with promising activities against the tested cells. Comparing to colchicine ($\text{IC}_{50} = 7.40, 9.32, \text{ and } 10.41\text{ }\mu\text{M}$ against HepG-2, HCT-116, and MCF-7, respectively), compounds **20**, **21**, **22**, **23**, **24**, **25**, **26**, and **28** exhibited superior cytotoxic activities with IC_{50} values ranging from 1.78 to $9.19\text{ }\mu\text{M}$. Taking compound **25** as demonstrative example, it showed 3.91, 6.51 and 2.47 times of colchicine cytotoxic activity against HepG-2, HCT-116, and MCF-7, respectively. Also, compound **20** exhibited 2.84, 5.15 and 2.30 times of colchicine activity against HCT-116, HepG-2, and MCF-7, respectively. In addition, Compounds **14**, **19**, **32**, and **33** exhibited superior activities against HCT-116 and MCF-7 with IC_{50} values ranging from 6.48 to $10.27\text{ }\mu\text{M}$.

Additionally, compounds **15**, **17**, **18**, **29**, and **34** displayed moderate anti-proliferative activities against all the tested cell lines with IC_{50} values ranging from 10.18 to $17.62\text{ }\mu\text{M}$. On the other hand, compounds **5**, **6**, **8**, **12**, and **30** showed weak anti-proliferative activities against all cell lines with IC_{50} values ranging from 22.43 to $45.53\text{ }\mu\text{M}$.

Finally, compound **16** showed strong activity against HCT-116, HepG-2 cell lines ($\text{IC}_{50} = 9.30$ and $8.87\text{ }\mu\text{M}$, respectively) and moderated activity against MCF-7 cells ($\text{IC}_{50} = 13.89\text{ }\mu\text{M}$). Compound **13** showed strong activity against HepG-2 cell line



Scheme 2. Synthesis of the target compounds 8–25.

($IC_{50} = 9.96 \mu M$) and moderated activity against HCT-116 and MCF-7 cells ($IC_{50} = 12.87$ and $17.04 \mu M$, respectively). Compounds **9** and **10** showed moderate activity against HCT-116 ($IC_{50} = 16.64$ and $15.38 \mu M$, respectively), HepG-2 ($IC_{50} = 17.40$ and $17.41 \mu M$, respectively) cell lines, and showed weak activity against MCF-7 cells ($IC_{50} = 20.49$ and $25.12 \mu M$, respectively).

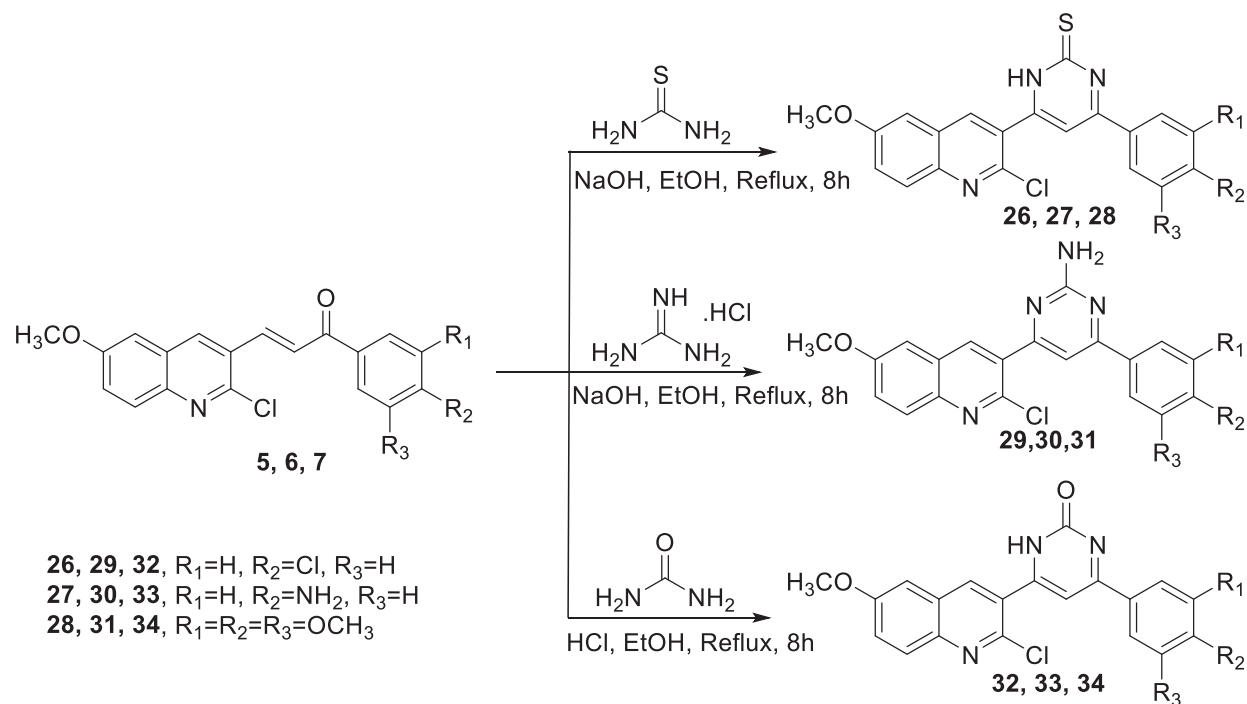
2.2.2. Tubulin polymerisation assay

The most active antiproliferative members were further evaluated for their inhibitory effect against tubulin polymerisation. The inhibition assay on microtubule polymerisation was evaluated turbidimetrically using a fluorescent plate reader⁴⁹. Colchicine and CA-4 were used as positive controls (Table 2).

Compounds **21** and **32** exhibited the highest tubulin polymerisation inhibitory effect with IC_{50} values of 9.11 and 10.5 nM, respectively. Such members showed activities higher than that of colchicine ($IC_{50} = 10.6$ nM) and CA-4 ($IC_{50} = 13.2$ nM). Moreover, compounds **20**, **22**, **25**, **26**, **28**, and **33** showed promising activities with IC_{50} values of 36.8, 19.1, 41.3, 34.5, 37.4 and 47.2 nM, respectively. Compounds **14** showed moderate activity with IC_{50} value of 50.1 nM. Finally, Compound **24** exhibited weak tubulin polymerisation inhibitory activity with IC_{50} value of 146.2 nM.

2.2.3. Cell cycle analysis

The impact of the most promising compound **25** on cell cycle distribution was assessed. Such analysis gave a better insight into the effect of the synthesised compounds on cancer cell growth



Scheme 3. Synthesis of the target compounds 26–34.

Table 1. *In vitro* anti-proliferative activities of the tested compounds and colchicine

Comp.	IC ₅₀ (μM) ^a		
	HepG-2	HCT-116	MCF-7
5	29.17 ± 1.9	28.92 ± 1.7	32.19 ± 2.0
6	32.91 ± 2.1	28.63 ± 1.7	37.31 ± 2.1
7	23.63 ± 1.3	25.08 ± 1.2	16.87 ± 1.2
8	30.92 ± 1.2	22.43 ± 1.1	33.53 ± 2.4
9	16.64 ± 0.8	17.40 ± 1.0	20.49 ± 1.1
10	15.38 ± 0.9	17.41 ± 1.1	25.12 ± 1.2
11	20.52 ± 1.0	19.72 ± 1.3	22.77 ± 1.4
12	35.44 ± 1.8	40.47 ± 2.4	45.53 ± 2.8
13	12.87 ± 0.6	9.96 ± 0.3	17.04 ± 1.2
14	8.92 ± 0.4	7.62 ± 0.4	10.04 ± 0.4
15	10.25 ± 0.4	11.56 ± 0.9	13.60 ± 0.7
16	9.30 ± 0.3	8.87 ± 0.3	13.89 ± 0.3
17	12.73 ± 0.5	11.42 ± 0.4	15.94 ± 0.6
18	10.18 ± 0.4	10.41 ± 0.3	13.70 ± 0.8
19	10.94 ± 0.5	7.38 ± 0.4	9.04 ± 0.5
20	2.60 ± 0.1	1.81 ± 0.1	4.51 ± 0.2
21	7.32 ± 0.2	8.91 ± 0.3	9.19 ± 0.3
22	4.76 ± 0.2	3.04 ± 0.3	6.45 ± 0.2
23	2.64 ± 0.1	1.78 ± 0.1	4.48 ± 0.1
24	3.14 ± 0.1	4.18 ± 0.2	4.97 ± 0.1
25	1.89 ± 0.2	1.43 ± 0.1	4.21 ± 0.1
26	3.62 ± 0.1	2.24 ± 0.2	5.55 ± 0.2
27	16.26 ± 0.4	22.36 ± 0.5	24.34 ± 0.9
28	5.47 ± 0.2	5.85 ± 0.3	7.34 ± 0.2
29	16.49 ± 0.8	13.04 ± 0.6	17.62 ± 0.8
30	28.53 ± 1.3	32.74 ± 0.9	33.75 ± 1.5
31	9.45 ± 0.5	10.49 ± 0.4	15.19 ± 0.7
32	8.16 ± 0.2	6.48 ± 0.2	9.89 ± 0.4
33	9.37 ± 0.4	8.50 ± 0.2	10.27 ± 0.5
34	15.27 ± 0.4	11.92 ± 0.4	15.44 ± 0.8
Colchicine	7.40 ± 0.2	9.32 ± 0.2	10.41 ± 0.3

^aIC₅₀ values are the mean ± SD of three separate experiments. Bold figures indicate superior potency than colchicine and CA-4.

inhibition. HepG-2 cells were utilised in this test. The reported method described by Wand et al.⁵⁰ was followed. HepG-2 cells were treated with compound **25** at a concentration equals its IC₅₀ value (1.89 μM) for 24 h.

The results revealed that compound **25** induced an increase in the percentage of HepG-2 cells from 24.83% to 28.95% at S phase. It exhibited marked increase in the percentage of HepG-2 cells from 13.8% to 30.17% at G2/M phase. Also, it increased the percentage of HepG-2 cells from 2.57% to 21.46% at Pre-G1 phase. On the other hand, it decreased the percentage of HepG-2 cells from 61.37% to 40.88% at G0-G1 phase. These findings indicated that compound **25** can arrest the cell cycle at G2/M phase, and can cause apoptosis at pre-G1 phase (Table 3 and Figure 8).

2.2.4. Annexin V-FITC apoptosis assay

Annexin V and PI double staining assay⁵¹ was carried out to explore the proposed apoptotic effect of the synthesised compounds. Compound **25** as a representative example was tested against HepG-2 cells. In this test, HepG-2 cells were incubated with compound **25** at a concentration of 1.89 μM for 24 h.

As shown in Table 4 and Figure 9, compound **25** induced apoptotic effect equal 19.05% (7.66% and 11.39 at early and late apoptosis, respectively), which was thirteen times more than the control (1.39%).

2.3. Docking studies

The synthesised compounds were docked against tubulin heterodimers using MOE2014 software to determine the binding free energy and binding mode (Table 5). Molecular docking studies gives perception about the binding mode and the degree of affinity between the docked compounds and the prospective target. good biological effect is shown by lower binding free energy and similar binding mode to that of the reference co-crystallised ligand.⁵²

A docking study of the co-crystallised ligand, DAMA-colchicine provides a binding energy value of -12.88 Kcal/mol with four hydrogen bonds and six hydrophobic interactions. The trimethoxy phenyl (A-ring) ring occupied the first pocket of the colchicine

binding site forming one hydrogen bond with Cys241. Other inter-actions were observed between the ring-A and different essential amino acid residues as Cys241, Leu255, and Ala250. Additionally, the side chain of the B-ring (2-mercaptoacetamide moiety) occupied the second cavity of the colchicine binding site forming two hydrogen bonds with Ser178 and Leu248. Furthermore, the methoxytropone moiety (C-ring) occupied the third pocket of the receptor forming one hydrogen and one hydrophobic bonds with Lys352 (Figure 10).

Compound **19** as a representative example showed a binding mode like that of DAMA-colchicine, with affinity value of -16.51 kcal/mol. The 3,4,5-trimethoxyphenyl moiety (A-ring) occupied the first cavity of the colchicine binding site forming three hydrophobic interactions with Ala250, Leu255, and Leu248. Additionally, the 2-acetyl-4,5-dihydro-1H-pyrazol moiety (B-ring) occupied the second cavity of the colchicine binding site forming one hydrogen bond with Asn258 and one hydrophobic interaction with Leu248. Furthermore, the 2-chloro-6-methoxyquinoline moiety (C-ring) occupied the third pocket of the colchicine binding site (Figure 11).

The binding mode of compound **25** exhibited an affinity value of -17.12 kcal/mol. The 3,4,5-trimethoxyphenyl moiety (A-ring) occupied the first cavity of the colchicine binding site forming one hydrophobic interaction with Leu248. The linker moiety

(1-(2,4-dinitrophenyl)-4,5-dihydro-1H-pyrazole) occupied the second cavity of the colchicine binding site forming five hydrogen bonds with Lys352, Ser178, and Asn258. Also, it formed three hydrophobic interactions with Lys352, Ala250 and Leu248. Furthermore, the 2-chloro-6-methoxyquinoline moiety (C-ring) occupied the third pocket of the colchicine binding site forming eight hydrophobic interactions with Leu255, Cys241, and Leu248 (Figure 12).

The binding mode of compound **28** exhibited an affinity value of -12.74 kcal/mol. The 3,4,5-trimethoxyphenyl moiety (A-ring) occupied the first cavity of the colchicine binding site forming four hydrophobic interactions with Ala316, Ala250, Cys241, and Leu255. The pyrimidine-2(1H)-thione (B-ring) occupied the second cavity of the colchicine binding site forming one hydrogen one hydrophobic bonds with Lys352. Furthermore, the 2-chloro-6-methoxyquinoline moiety (C-ring) occupied the third pocket of the colchicine binding site forming three hydrophobic interactions with Lys254 and Ala180. The methoxy group formed one hydrogen bond with Gln11 (Figure 13).

2.4. Structure-activity relationship (SAR)

SAR as an aim of our work was based on the results of *in vitro* cytotoxic activities of the synthesised compounds. Initially, the effect of the A-ring on the activity was explored. Comparing the cytotoxic activity of compounds **22**, **25**, **28**, **31**, and **34** incorporating 4-methoxyphenyl as an A-ring with compounds **20**, **23**, **26**, **29**, and **32** incorporating 4-chlorophenyl as an A-ring, and compound **21**, **24**, **27**, **30**, and **32** incorporating 4-aminophenyl as an A-ring indicated that the cytotoxic activities decreased in the order of 4-methoxyphenyl > 4-chlorophenyl > 4-aminophenyl.

Then, the impact of the B-ring (linker region) was investigated. The increased IC_{50} values of compounds **5**, **6**, and **7** incorporated open structure at the linker region than those of their corresponding members incorporating cyclic structure, indicated that

Table 2. *In vitro* tubulin polymerisation inhibition.

Comp.	IC ₅₀ (nM) ^a Tubulin polymerisation inhibition	Comp.	IC ₅₀ (nM) ^a Tubulin polymerisation inhibition
14	50.1	26	34.5
20	36.8	28	37.4
21	9.11	32	10.5
22	19.1	33	47.2
24	146.2	Colchicine	10.6
25	41.3	CA-4	13.2

^aIC₅₀ values are the mean \pm SD of three separate experiments.

Table 3. Effect of compound **25** on cell cycle progression in HepG-2 cells.

Sample	Cell cycle distribution (%)			
	%G0-G1	%S	%G2-M	%Pre-G1
25 / HepG-2	40.88	28.95	30.17	21.46
Cont. HepG-2	61.37	24.83	13.8	2.57

Table 4. Apoptosis and necrosis percent induced by compound **25** in HepG-2 cells.

Sample	Apoptosis			Necrosis
	Total	Early	Late	
25 / HepG-2	21.46	7.66	11.39	2.41
Cont. HepG-2	2.57	0.67	0.72	1.18

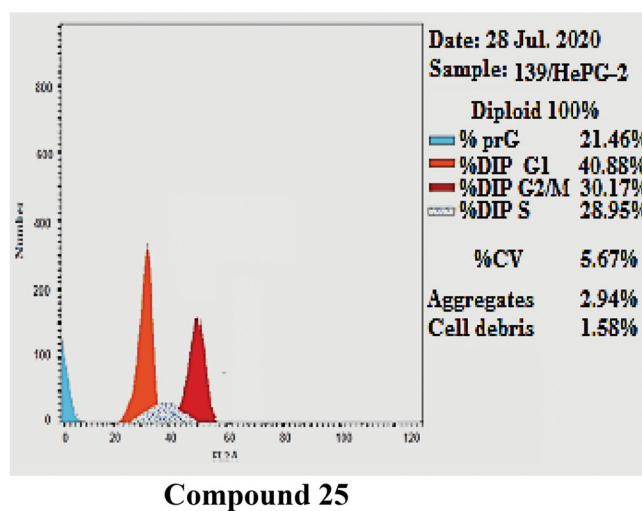
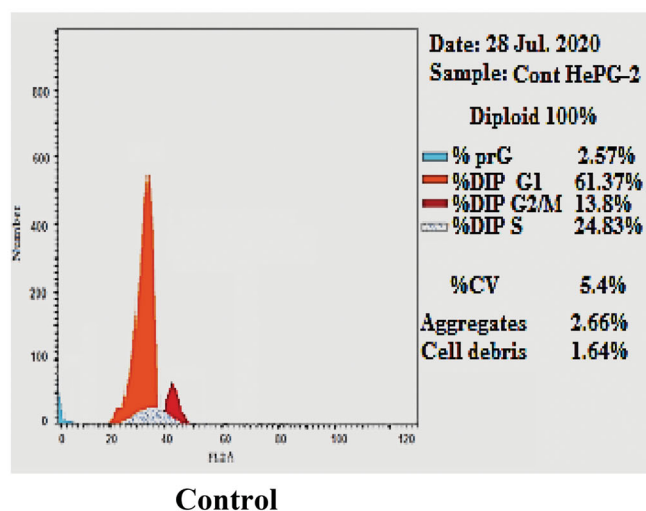


Figure 8. HepG-2 cells distribution upon treatment with compound **25**.

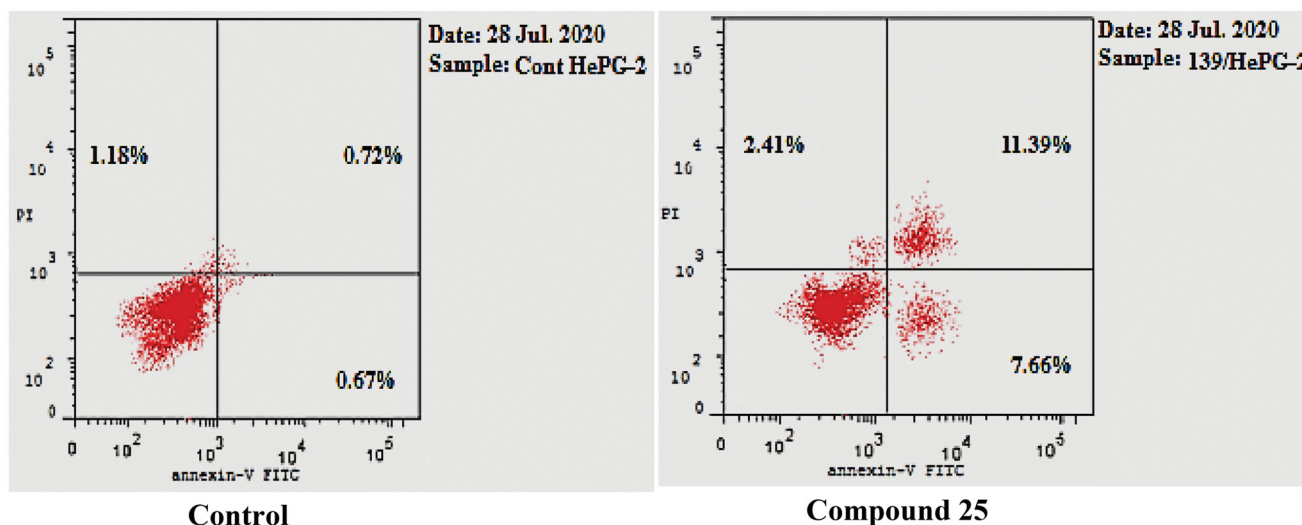


Figure 9. Induced apoptosis on HepG-2 cells by compound 25.

Table 5. The docking scores of the synthesised compounds, colchicine, and co-crystallised ligand (DAMA-colchicine) against tubulin

Comp.	Binding free energy (kcal/mol)	Comp.	Binding free energy (kcal/mol)
5	-9.95	21	-11.67
6	-10.04	22	-14.72
7	-13.48	23	-13.42
8	-10.23	24	-14.35
9	-10.71	25	-17.12
10	-14.02	26	-11.23
11	-10.20	27	-11.25
12	-10.47	28	-12.74
13	-13.73	29	-11.18
14	-13.28	30	-11.11
15	-11.63	31	-14.65
16	-14.62	32	-11.05
17	-12.07	33	-11.02
18	-11.89	34	-13.14
19	-16.51	DAMA-colchicine	-12.88
20	-12.35	Colchicine	-13.45

cyclisation of the linker region (B-ring) is advantageous. For the B-ring, the cytotoxic activities decreased in the order of substituted five-membered ring (compounds **14–25**) > non-substituted six-membered ring (compounds **26–34**) > non-substituted five-membered ring (compounds **8–13**). With regard to the substituted five-membered ring, it was found that the cytotoxicity decrease in the order of 2,4-dinitrophenyl (compounds **23–25**) > phenyl (compounds **20–22**) > ethane-1-thione (compounds **14–16**) > ethan-1-one (compounds **17–19**).

For the non-substituted five-membered ring, it was found 4,5-dihydro-1H-pyrazole derivatives (compounds **8–9**) are almost equipotent with 4,5-dihydroisoxazole ones (compounds **11–13**). For the non-substituted six-membered ring, it was found pyrimidine-2(1H)-thione derivatives (compounds **26–28**) are more active than 2-amino pyrimidine derivatives (compounds **29–31**), which were more active than pyrimidin-2(1H)-one derivatives (compounds **32–34**) (Figure 14).

3. Conclusion

In summary, twenty-nine of quinoline derivatives were designed and synthesised. The synthesised compounds were evaluated for their anti-proliferative activities against a group of three human

cancer cell lines including; colorectal carcinoma (HCT-116), hepatocellular carcinoma (HepG-2), and breast cancer (MCF-7). Compounds **20**, **21**, **22**, **23**, **24**, **25**, **26**, and **28** exhibited superior cytotoxic activities with IC_{50} values ranging from 1.78 to 9.19 μ M. Additionally, the most promising members were tested for their tubulin polymerisation inhibitory effect. Compounds **21** and **32** exhibited the highest tubulin polymerisation inhibitory effect with IC_{50} values of 9.11 and 10.5 nM, respectively. Structure-activity relationship of the synthesised compounds revealed that 4-methoxyphenyl > 4-chlorophenyl > 4-aminophenyl as an A-ring. In the same time. The it was found that substituted five-membered ring > non-substituted six-membered ring > non-substituted five-membered ring as a B-ring. Moreover, compound **25** was approved to arrested the cell cycle at the G2/M phase and induced apoptosis in HepG-2 cells. Docking experiments assisted these findings by anticipating potential binding interactions between the target compounds and the active sites of tubulin heterodimers. The most effective candidates in the quest for strong and selective antineoplastic agents will serve as valuable lead compounds and merit further investigations.

4. Experimental

4.1. Chemistry

1H NMR spectra were run at 400 MHz and ^{13}C spectra were determined at 100 MHz in deuterated chloroform ($CDCl_3$), or dimethyl sulfoxide ($DMSO-d_6$) on a Varian Mercury VX-400 NMR spectrometer. Chemical shifts are given in parts per million (ppm) on the delta (δ) scale. Chemical shifts were calibrated relative to those of the solvents. Flash chromatography was performed on 230–400 mesh silica. The progress of reactions was monitored with Merck silica gel IB2-F plates (0.25 mm thickness). The infra-red spectra were recorded in potassium bromide discs on pye Unicam SP 3300 and Shimadzu FT IR 8101 PC infra-red spectrophotometer. Mass spectra were recorded at 70 eV. High resolution mass spectra for all ionisation techniques were obtained from a Finnigan MAT XL95. Melting points were determined using capillary tubes with a Stuart SMP30 apparatus and are uncorrected. All yields reported refer to isolated yields.

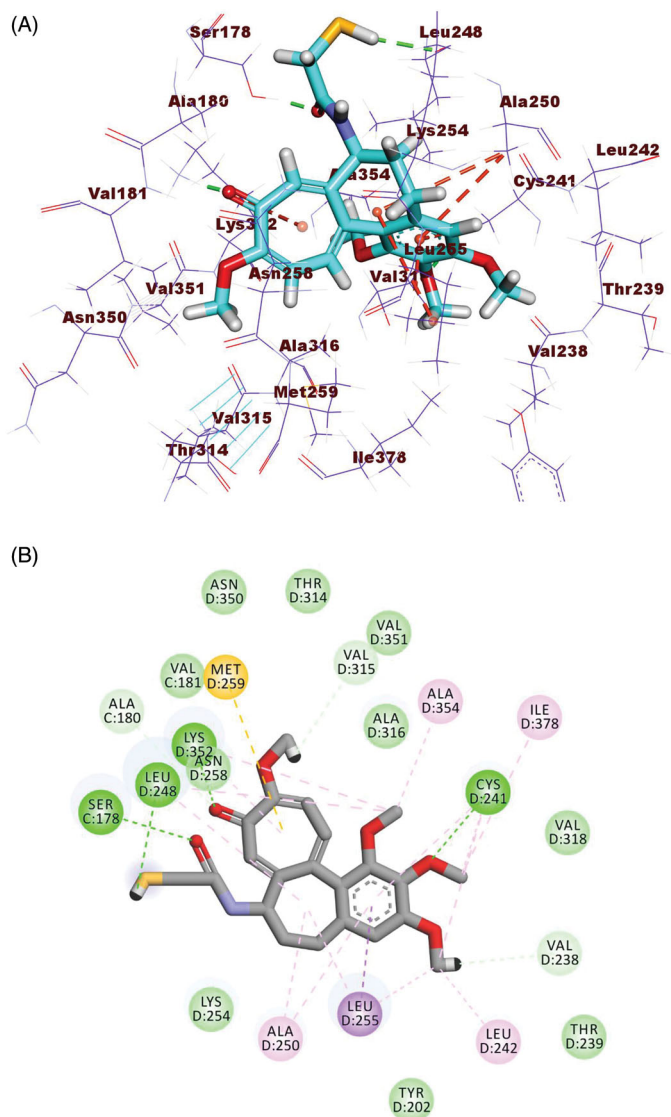


Figure 10. (A) 3D structure of co-crystallised ligand, DAMA-colchicine, docked into the colchicine binding site (B) 2D structure of co-crystallised ligand, DAMA-colchicine, docked into the colchicine binding site.

4.1.1. General procedure for synthesis of compounds (5, 6, and 7)

To a stirred and ice-cooled aqueous solution of sodium hydroxide (10 mmole, 50% w/w) and absolute ethanol (12.5 mL), substituted acetophenone (10 mmole) namely, 4-chloroacetophenone, 4-aminoacetophenone, and 3,4,5-trimethoxyacetophenone was added followed by 2-chloro-6-methoxyquinoline-3-carbadehyde **4** (10 mmole). The reaction mixture was vigorously stirred for 3–6 h while temperature was maintained below 25 °C till the reaction mixture became thick. The reaction mixture was left in the refrigerator overnight. The formed precipitate was filtered off under vacuum and washed with copious amount of water until the filtrates became neutral to litmus paper, washed with ice-cold ethanol (20 mL), and then recrystallized from ethanol to give the titled compound **5**, **6**, and **7**, respectively.

4.1.1.1. (E)-3-(2-Chloro-6-methoxyquinolin-3-yl)-1-(4-chlorophenyl)prop-2-en-1-one (5). Yellow solid (93%) mp = 135–136 °C; IR (KBr) cm^{-1} : 3080 (CH aromatic), 2900 (CH aliphatic), 1655 (C=O); $^1\text{H NMR}$ (DMSO- d_6) δ : 9.10 (s, 1H, quinoline-H4), 8.20 (d, $J = 8.4$ Hz, 2H, phenyl-H2, H6 protons), 8.13 (d, $J = 15.2$, 1H, CH alkene β proton), 7.96 (d, $J = 15.2$ Hz, 1H, CH alkene α proton), 7.92 (d, $J = 9.2$,

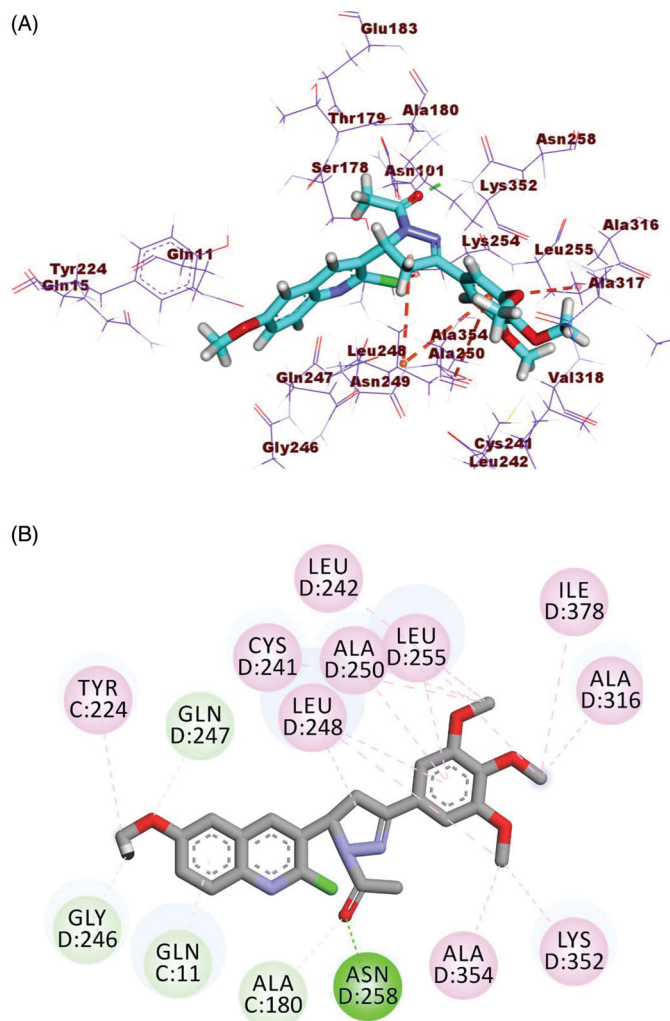


Figure 11. (A) 3D structure of compound 19 docked into the colchicine binding site (B) 2D structure of compound 19 docked into the colchicine binding site.

1H, quinoline-H8), 7.50 (d, $J = 9.2$ Hz, 1H, quinoline-H7), 7.39 (s, 1H, quinoline-H5), 7.14 (d, $J = 8.4$, 2H, phenyl-H3, H5 protons), 3.87 (s, 3H, quinoline-OCH₃); MS (m/z) 361 (0.8%, M + 4), 359 (4.3%, M + 2), 357 (6.7%, M⁺), 246 (61%), 138 (100%); Anal. Calc. for: (C₁₉H₁₃Cl₂NO₂): C, 63.71; H, 3.66; N, 3.91%; Found: C, 63.74; H, 3.71; N, 3.97%.

4.1.1.2. (E)-1-(4-Aminophenyl)-3-(2-chloro-6-methoxyquinolin-3-yl)prop-2-en-1-one (6). Orange solid (89%) mp = 120–121 °C; IR (KBr) cm^{-1} : 3310, 3295 (NH₂), 3054 (CH aromatic), 2962 (CH aliphatic), 1653 (C=O); $^1\text{H NMR}$ (DMSO- d_6) δ : 9.08 (s, 1H, quinoline-H4), 8.07 (d, $J = 15.2$ Hz, 1H, CH alkene β proton), 7.96 (d, $J = 8.8$, 2H, phenyl-H2, H6 protons), 7.92 (d, $J = 15.2$ Hz, 1H, CH alkene α proton), 7.88 (d, $J = 9.2$, 1H, quinoline-H8), 7.49 (d, $J = 9.2$ Hz, 1H, quinoline-H7), 7.38 (s, 1H quinoline-H5), 6.64 (d, $J = 8.8$, 2H, phenyl-H3, H5 protons), 6.25 (brs, 2H, NH₂, D₂O-exchangeable), 3.91 (s, 3H, quinoline-OCH₃); MS (m/z) 340 (1.96%, M⁺ + 2), 338 (5.8%, M⁺), 246 (66%), 120 (100%); Anal. Calc. for: (C₁₉H₁₅ClN₂O₂): C, 67.36; H, 4.46; N, 8.27%; Found: C, 67.41; H, 4.49; N, 8.31%.

4.1.1.3. (E)-3-(2-Chloro-6-methoxyquinolin-3-yl)-1-(3,4,5-trimethoxyphenyl)prop-2-en-1-one (7). Yellow solid (91%) mp = 127–128 °C; IR (KBr) cm^{-1} : 3064 (CH aromatic), 2910 (CH aliphatic), 1655 (C=O); $^1\text{H NMR}$ (DMSO- d_6) δ : 9.12 (s, 1H, quinoline-H4), 8.16 (d,

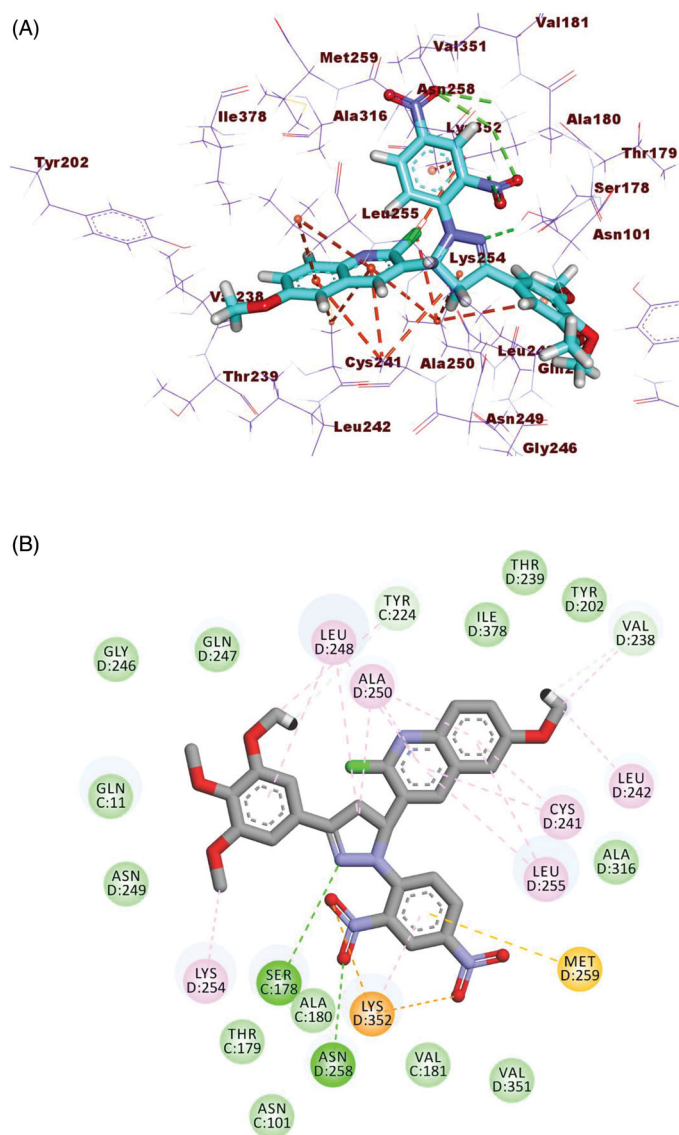


Figure 12. (A) 3D structure of compound 25 docked into the colchicine binding site (B) 2D structure of compound 25 docked into the colchicine binding site.

$J = 15.3\text{ Hz}$, 1H, CH alkene β proton), 8.02 (d, $J = 15.3$, 1H, CH alkene α proton), 7.91 (d, $J = 9.3\text{ Hz}$, 1H, quinoline-H8), 7.52 (d, $J = 9.3\text{ Hz}$, 1H, quinoline-H7), 7.41 (s, 1H, quinoline-H5), 7.14 (s, 2H, phenyl-H2, H6 protons), 3.94 (s, 6H, 2OCH_3), 3.89 (s, 6H, 2OCH_3); MS (m/z) 415 (2.7%, $M^+ + 2$), 413 (7.8%, M^+), 246 (76%), 195 (100%); Anal. Calc. for: ($\text{C}_{22}\text{H}_{20}\text{ClNO}_5$): C, 63.85; H, 4.87; N, 3.38%; Found: C, 63.92; H, 4.92; N, 3.40%.

4.1.2. General procedure for synthesis of compounds (8–25)

A mixture of chalcone **5–7** (10 mmole) and the appropriate amine derivatives namely, hydrazine hydrate, hydroxylamine hydrochloride, thiosemicarbazide, semicarbazide, phenylhydrazine, 2,4-dinitrophenylhydrazine (10 mmole) were stirred in ethanol (20 mL), and then sodium hydroxide (0.8 g, 20 mmole), in case of hydroxylamine hydrochloride, was added. The reaction mixture was heated to reflux for 7–12 h, and then the solvent was evaporated under reduced pressure and poured into ice water. The obtained precipitate was filtered off, washed with copious amount of water and

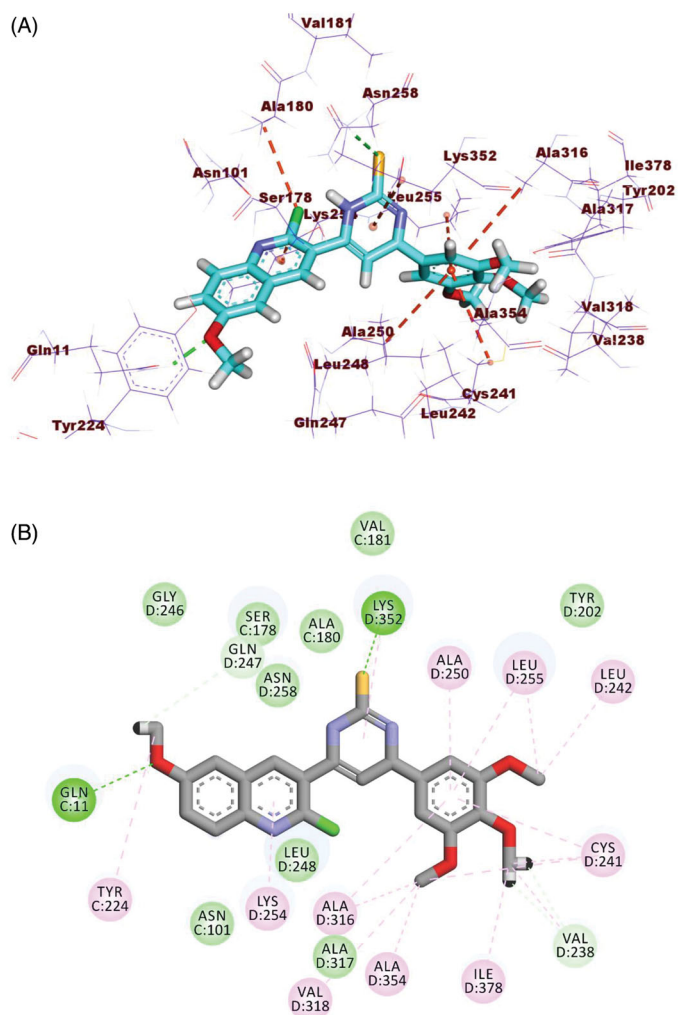


Figure 13. (A) 3D structure of compound 28 docked into the colchicine binding site (B) 2D structure of compound 28 docked into the colchicine binding site.

recrystallized from ethanol to afford the corresponding compounds **8–25**.

4.1.2.1. 2-Chloro-3-[3-(4-chlorophenyl)-4,5-dihydro-1H-pyrazol-5-yl]-6-methoxyquinoline (8). White solid (76%) mp = 118–119 °C; IR (KBr) cm^{-1} : 3295 (NH), 3071 (CH aromatic), 2945 (CH aliphatic); ^1H NMR ($\text{DMSO-}d_6$) δ : 8.40 (s, 1H, quinoline-H4), 7.84 (d, $J = 8.8\text{ Hz}$, 2H, phenyl-H2, H6 protons), 7.62 (d, $J = 9.6$, 1H, quinoline-H8), 7.46 (s, 1H, quinoline-H5), 7.41 (d, $J = 9.6\text{ Hz}$, 1H, quinoline-H7), 7.01 (brs, 1H, NH, D_2O -exchangeable), 6.94 (d, $J = 8.8$, 2H phenyl-H3, H5 protons), 5.13 (t, $J = 10\text{ Hz}$, 1H, pyrazole-H5), 3.75 (s, 3H, quinoline- OCH_3), 3.70 (dd, $J = 5.6$, $J = 16.8$, 1H, pyrazole- H4 axial proton), 2.89 (dd, $J = 9.6$, $J = 16.4$, 1H, pyrazole-H4 equatorial proton); ^{13}C NMR ($\text{DMSO-}d_6$) δ : 159.4, 153.4, 147.9, 144.4, 142.3, 134.2, 133.2, 130.5, 129.3, 129.1, 128.1, 126.4, 123.8, 106.5, 55.9, 50.6, 46.1; MS (m/z) 375 (0.8%, $M^+ + 4$), 373 (4.3%, $M + 2$), 371 (6.7%, M^+), 179 (61%), 192 (100%); Anal. Calc. for: ($\text{C}_{19}\text{H}_{15}\text{Cl}_2\text{N}_3\text{O}$): C, 61.31; H, 4.06; N, 11.29%; Found: C, 61.35; H, 4.11; N, 11.35%.

4.1.2.2. 4-[5-(2-Chloro-6-methoxyquinolin-3-yl)-4,5-dihydro-1H-pyrazol-3-yl]aniline (9). Yellow solid (81%) mp = 122–123 °C; 3305, 2984 (NH_2), 3045 (CH aromatic), 2935 (CH aliphatic); ^1H NMR ($\text{DMSO-}d_6$) δ : 10.02 (brs, 1H, NH, D_2O -exchangeable), 8.39 (s, 1H, quinoline-H4), 7.84 (d, $J = 9.2\text{ Hz}$, 1H, quinoline-H8), 7.48 (s, 1H, quinoline-H5), 7.45 (d, $J = 9.2$, 1H, quinoline-H7), 7.32 (d, $J = 8.8\text{ Hz}$,

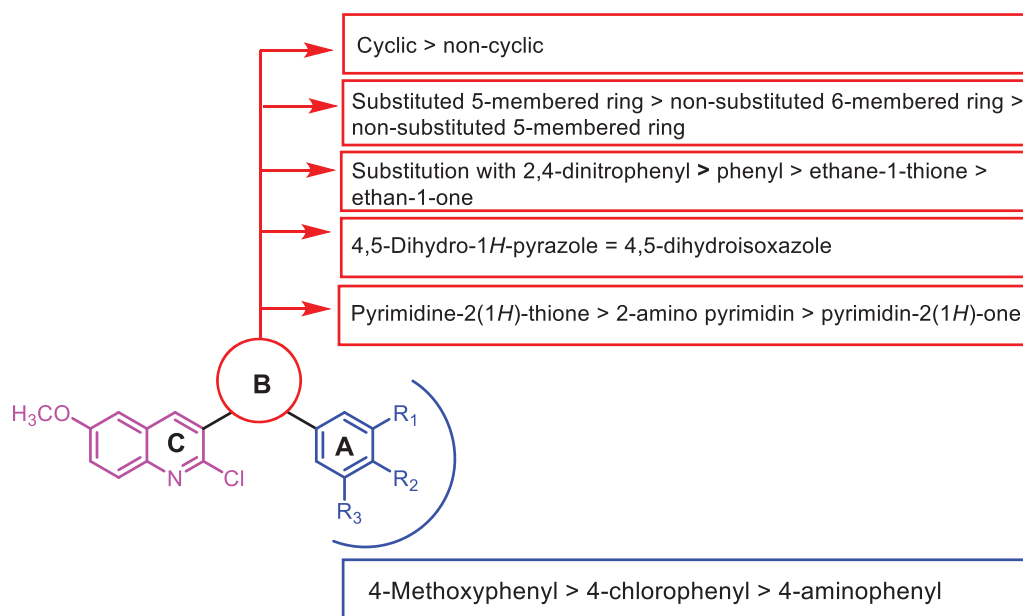


Figure 14. Structure-activity relationship of the synthesised compounds as anti-proliferative agents.

2H, phenyl-H2, H6 protons), 6.55 (d, $J=8.8$ Hz, 2H, phenyl-H3, H5 protons), 5.36 (brs, 2H, NH₂, D₂O-exchangeable), 5.04 (t, $J=10$ Hz, 1H, pyrazole-H5), 3.85 (s, 3H, quinoline-OCH₃), 3.57 (dd, $J=10.8$ Hz, $J=16.4$ Hz, 1H, pyrazole-H4 axial proton), 2.77 (dd, $J=10$ Hz, $J=16.4$ Hz, 1H, pyrazole-H4 equatorial proton); ¹³C NMR (DMSO-*d*₆) δ : 159.4, 153.4, 150.3, 148.9, 142.3, 139.2, 135.7, 131.9, 129.4, 127.7, 127.1, 121.8, 116.6, 106.9, 55.2, 43.7, 36.7; MS (*m/z*) 354 (5.9%, M + 2), 352 (18%, M⁺), 260 (46%), 192 (100%); Anal. Calc. for: (C₁₉H₁₇ClN₄O): C, 64.68; H, 4.86; N, 15.88%; Found: C, 64.73; H, 4.91; N, 15.92%.

4.1.2.3. 2-Chloro-6-methoxy-3-[3-(3,4,5-trimethoxyphenyl)-4,5-dihydro-1H-pyrazol-5-yl]quinoline (10). Yellow solid (77%) mp = 114–115 °C; 3295 (NH), 3047 (CH aromatic), 2944 (CH aliphatic); ¹H NMR (DMSO-*d*₆) δ : 8.41 (s, 1H, quinoline-H4), 7.86 (d, $J=9.2$ Hz, 1H, quinoline-H8), 7.55 (s, 2H, phenyl-H2, H6 protons), 7.54 (brs, 1H, NH, D₂O-exchangeable), 7.48 (s, 1H, quinoline-H5), 7.43 (d, $J=9.2$ Hz, 1H, quinoline-H7), 5.14 (t, $J=9.2$ Hz, 1H, pyrazole-H5), 3.87 (s, 6H, 2OCH₃), 3.76 (s, 6H, 2OCH₃), 3.66 (dd, $J=11.2$ Hz, $J=16.4$ Hz, 1H, pyrazole-H4 axial proton), 2.87 (dd, $J=9.2$ Hz, $J=16.4$ Hz, 1H, pyrazole-H4 equatorial proton); ¹³C NMR (DMSO-*d*₆) δ : 157.9, 153.8, 153.4, 149.6, 144.7, 142.4, 136.8, 133.0, 128.1, 127.7, 126.4, 123.6, 115.3, 106.5, 56.9, 55.5, 55.1, 37.8, 29.9; MS (*m/z*) 429 (15%, M + 2), 427 (46%, M⁺), 192 (100%); Anal. Calc. for: (C₂₂H₂₂ClN₃O₄): C, 61.76; H, 5.18; N, 9.82%; Found: C, 61.82; H, 5.22; N, 9.84%.

4.1.2.4. 5-(2-Chloro-6-methoxyquinolin-3-yl)-3-(4-chlorophenyl)-4,5-dihydroisoxazole (11). Yellow solid (64%) mp = 145–146 °C; 3031 (CH aromatic), 2957 (CH aliphatic), 1590 (C=N); ¹H NMR (DMSO-*d*₆) δ : 8.31 (s, 1H, quinoline-H4), 7.88 (d, $J=8.8$ Hz, 2H, phenyl-H2, H6 protons), 7.65 (d, $J=9.6$ Hz, 1H, quinoline-H8), 7.51 (s, 1H, quinoline-H5), 7.43 (d, $J=9.6$ Hz, 1H, quinoline-H7), 6.99 (d, $J=8.8$ Hz, 2H, phenyl-H3, H5 protons), 6.02 (dd, $J=6.8$ Hz, $J=11.2$ Hz, 1H, isoxazole-H5), 4.08 (dd, $J=11.2$ Hz, $J=16.8$ Hz, 1H, isoxazole-H4 axial proton), 3.78 (s, 3H, quinoline OCH₃), 3.51 (dd, $J=6.8$ Hz, $J=17.2$ Hz, 1H, isoxazole-H4 equatorial proton); ¹³C NMR (DMSO-*d*₆) δ : 159.7, 153.4, 149.3, 145.1, 142.3, 134.3, 133.3, 130.5, 129.1, 128.1, 127.4, 126.0, 123.6, 106.2, 59.0, 55.5, 45.4; MS (*m/z*) 377 (1.8%, M + 4),

375 (12.3%, M + 2), 373 (18.9%, M⁺), 180 (100%); Anal. Calc. for: (C₁₉H₁₄Cl₂N₂O₂): C, 61.14; H, 3.78; N, 7.51%; Found: C, 61.16; H, 3.81; N, 7.54%.

4.1.2.5. 4-[5-(2-Chloro-6-methoxyquinolin-3-yl)-4,5-dihydroisoxazol-3-yl]aniline (12). Orange solid (61%) mp = 127–128 °C; 3300, 3104 (NH₂), 3041 (CH aromatic), 2959 (CH aliphatic); ¹H NMR (DMSO-*d*₆) δ : 8.26 (s, 1H, quinoline-H4), 7.84 (d, $J=9.2$ Hz, 1H, quinoline-H8), 7.53 (s, 1H, quinoline-H5), 7.42 (d, $J=9.2$ Hz, 1H, quinoline-H7), 7.36 (d, $J=8.8$ Hz, 2H, phenyl-H2, H6 protons), 6.55 (d, $J=8.8$ Hz, 2H, phenyl-H3, H5 protons), 5.93 (t, $J=6$ Hz, 1H, isoxazole-H5), 5.62 (brs, 2H, NH₂, D₂O-exchangeable), 3.96 (dd, $J=10.8$ Hz, $J=17.2$ Hz, 1H, isoxazole-H4 axial proton), 3.85 (s, 3H, quinoline OCH₃), 3.38 (dd, $J=6.8$ Hz, $J=17.2$ Hz, 1H, isoxazole-H4 equatorial proton); ¹³C NMR (DMSO-*d*₆) δ : 162.4, 159.0, 150.6, 148.6, 142.7, 139.5, 136.1, 129.4, 128.4, 127.7, 127.1, 121.8, 116.6, 106.5, 59.0, 55.5, 38.5; MS (*m/z*) 355 (7.3%, M⁺ + 2), 353 (23.1%, M⁺), 161 (37%), 192 (100%); Anal. Calc. for: (C₁₉H₁₆ClN₃O₂): C, 64.50; H, 4.56; N, 11.88%; Found: C, 64.54; H, 4.59; N, 11.91%.

4.1.2.5. 5-(2-Chloro-6-methoxyquinolin-3-yl)-3-(3,4,5-trimethoxyphenyl)-4,5-dihydroisoxazole (13). Red solid (59%) mp = 133–134 °C; 3062 (CH aromatic), 2978 (CH aliphatic); ¹H NMR (DMSO-*d*₆) δ : 8.32 (s, 1H, quinoline-H4), 7.87 (d, $J=9$ Hz, 1H, quinoline-H8), 7.67 (s, 2H, phenyl-H2, H6 protons), 7.53 (s, 1H, quinoline-H5), 7.44 (d, $J=9$ Hz, 1H, quinoline-H8), 6.02 (t, $J=6.9$ Hz, 1H, isoxazole-H5), 4.05 (dd, $J=5.2$ Hz, $J=11.1$ Hz, 1H, isoxazole-H4 axial proton), 3.87 (s, 6H, 2OCH₃), 3.79 (s, 6H, 2OCH₃), 3.52 (dd, $J=4.8$ Hz, $J=17.4$ Hz, 1H, isoxazole-H4 equatorial proton); ¹³C NMR (DMSO-*d*₆) δ : 162.1, 157.9, 153.4, 149.3, 144.4, 142.3, 136.5, 133.0, 128.1, 127.7, 126.4, 123.2, 115.6, 106.5, 61.8, 56.9, 55.2, 54.8, 31.2; MS (*m/z*) 430 (12%, M⁺ + 2), 428 (35%, M⁺), 192 (100%); Anal. Calc. for: (C₂₂H₂₁ClN₃O₅): C, 61.61; H, 4.94; N, 6.53%; Found: C, 61.66; H, 5.01; N, 6.54%.

4.1.2.6. 5-(2-Chloro-6-methoxyquinolin-3-yl)-3-(4-chlorophenyl)-4,5-dihydro-1H-pyrazole-1-carbothioamide (14). Yellow solid (65%) mp = 136–137 °C; 3310, 3249 (NH₂), 3031 (CH aromatic), 2974 (CH aliphatic); ¹H NMR (DMSO-*d*₆) δ : 8.56 (s, 1H, quinoline-H4), 8.40 (d,

$J=8.4$ Hz, 2H, phenyl-H2, H6 protons), 8.10 (d, $J=9.4$, 1H, quinoline-H8), 8.05 (s, 1H, quinoline-H5), 8.0 (brs, 2H, NH₂, D₂O-exchangeable), 7.95 (d, $J=9.2$ Hz, 1H, quinoline-H7), 6.96 (d, $J=8.4$, 2H, phenyl-H2, H6 protons), 4.57 (t, $J=7.6$ Hz, 1H, pyrazole-H5), 3.75 (s, 3H, quinoline OCH₃), 3.58 (dd, $J=12$, $J=16.8$, 1H, pyrazole-H4 axial proton), 2.93 (dd, $J=12$, $J=18.2$, 1H, pyrazole-H4 equatorial proton); ¹³C NMR (DMSO-*d*₆) δ : 179.8, 159.4, 153.8, 147.9, 144.7, 142.7, 134.3, 133.0, 130.5, 129.2, 128.1, 127.4, 126.4, 123.6, 106.5, 62.4, 55.9, 37.1; MS (*m/z*) 435 (1.2%, M+4), 433 (9%, M⁺+2), 431 (13.2%, M⁺), 192 (100%); Anal. Calc. for: (C₂₀H₁₆Cl₂N₄O₅): C, 55.69; H, 3.74; N, 12.99%; Found: C, 55.76; H, 3.82; N, 13.03%.

4.1.2.7. 3-(4-Aminophenyl)-5-(2-chloro-6-methoxyquinolin-3-yl)-4,5-dihydro-1H-pyrazole-1-carbothioamide (15). Orange solid (66%) mp = 123–124 °C; IR (KBr) cm⁻¹: 3300, 3251 (NH₂), 3037 (CH aromatic), 2898 (CH aliphatic); ¹H NMR (DMSO-*d*₆) δ : 8.22 (s, 1H, quinoline-H4), 7.83 (d, $J=9.2$ Hz, 1H, quinoline-H8), 7.73 (brs, 2H, NH₂, D₂O-exchangeable), 7.54 (d, $J=8.8$, 2H, phenyl-H2, H6 protons), 7.44 (s, 1H, quinoline-H5), 7.38 (d, $J=9.2$ Hz, 1H, quinoline-H7), 6.55 (d, $J=8.8$ Hz, 2H, phenyl-H3, H5 protons), 5.70 (brs, 2H, NH₂, D₂O-exchangeable), 5.14 (dd, $J=3.2$ Hz, $J=11.2$ Hz, 1H, pyrazole-H5), 3.94 (dd, $J=11.2$ Hz, $J=18.4$ Hz, 1H, pyrazole-H4 axial proton), 3.83 (s, 3H, quinoline OCH₃), 3.19 (dd, $J=3.2$ Hz, $J=17.6$ Hz, 1H, pyrazole-H4 equatorial proton); ¹³C NMR (DMSO-*d*₆) δ : 165.9, 159.3, 153.5, 150.6, 148.3, 142.3, 139.2, 137.1, 129.4, 128.1, 127.7, 126.7, 121.8, 116.4, 106.5, 64.9, 55.2, 36.8; MS (*m/z*) 413 (7.3%, M⁺+2), 411 (22%, M⁺), 219 (33%), 192 (100%); Anal. Calc. for: (C₂₀H₁₈ClN₅O₅): C, 58.32; H, 4.40; N, 17.0%; Found: C, 58.35; H, 4.44; N, 17.03%.

4.1.2.8. 5-(2-Chloro-6-methoxyquinolin-3-yl)-3-(3,4,5-trimethoxyphenyl)-4,5-dihydro-1H-pyrazole-1-carbothioamide (16). Yellow solid (69%) mp = 121–122 °C; IR (KBr) cm⁻¹: 3301, 3145 (NH₂), 3064 (CH aromatic), 2987 (CH aliphatic); ¹H NMR (DMSO-*d*₆) δ : 9.44 (brs, 2H, NH₂, D₂O-exchangeable), 8.39 (s, 1H, quinoline-H4), 7.57 (d, $J=9.2$ Hz, 1H, quinoline-H8), 7.57 (s, 2H, phenyl-H2, H6 protons), 7.44 (s, 1H, quinoline-H5), 7.44 (s, 1H, quinoline-H5), 6.94 (d, $J=9.2$ Hz, 1H, quinoline-H7), 5.12 (t, $J=10$ Hz, 1H, 1H, pyrazole-H5), 3.86 (s, 6H, 2OCH₃), 3.75 (s, 6H, 2OCH₃), 3.66 (dd, $J=10.8$ Hz, $J=16.4$ Hz, 1H, pyrazole-H4 axial proton), 2.84 (dd, $J=9.6$ Hz, $J=16.8$ Hz, 1H, pyrazole-H4 equatorial proton); ¹³C NMR (DMSO-*d*₆) δ : 169.0, 157.9, 155.5, 153.1, 149.3, 144.1, 142.7, 136.4, 133.0, 127.7, 127.1, 125.6, 123.9, 120.5, 106.2, 62.4, 57.9, 55.2, 54.8, 36.0; MS (*m/z*) 488 (22%, M⁺+2), 486 (65%, M⁺), 167 (100%); Anal. Calc. for: (C₂₃H₂₃ClN₄O₅S): C, 56.73; H, 4.76; N, 11.51%; Found: C, 56.80; H, 4.78; N, 11.53%.

4.1.2.9. 5-(2-Chloro-6-methoxyquinolin-3-yl)-3-(4-chlorophenyl)-4,5-dihydro-1H-pyrazole-1-carboxamide (17). White solid (58%) mp = 135–136 °C; IR (KBr) cm⁻¹: 3294, 3195 (NH₂), 3024 (CH aromatic), 2972 (CH aliphatic), 1681 (C=O); ¹H NMR (DMSO-*d*₆) δ : 8.57 (s, 1H, quinoline-H4), 8.51 (d, $J=5.2$ Hz, 2H, phenyl-H2, H6 protons), 8.93–8.04 (m, 3H quinoline-H5, H7 and H8), 7.93 (brs, 2H, NH₂, D₂O-exchangeable), 7.19 (d, $J=5.2$ Hz, 2H, phenyl-H3, H5 protons), 4.61 (t, $J=10$ Hz, 1H, pyrazole-H5), 3.74 (s, 3H, quinoline OCH₃), 3.57 (dd, $J=11.6$, $J=19.6$, 1H, pyrazole-H4 axial proton), 2.87 (dd, $J=8.4$, $J=17.6$, 1H, pyrazole-H4 equatorial proton); ¹³C NMR (DMSO-*d*₆) δ : 166.3, 160.1, 153.5, 146.5, 144.4, 141.2, 134.3, 133.0, 130.5, 129.1, 128.1, 127.4, 126.0, 123.9, 106.2, 59.0, 55.9, 36.0; MS (*m/z*) 419 (2.2%, M+4), 417 (14%, M⁺+2), 415 (22.2%,

M⁺), 192 (100%); Anal. Calc. for: (C₂₀H₁₆Cl₂N₄O₂): C, 57.85; H, 3.88; N, 13.49%; Found: C, 57.89; H, 3.94; N, 13.55%.

4.1.2.10. 3-(4-Aminophenyl)-5-(2-chloro-6-methoxyquinolin-3-yl)-4,5-dihydro-1H-pyrazole-1-carboxamide (18). Yellow solid (73%) mp = 130–131 °C; IR (KBr) cm⁻¹: 3298, 3193 (NH₂), 3056 (CH aromatic), 2983 (CH aliphatic), 1680 (C=O); ¹H NMR (DMSO-*d*₆) δ : 8.23 (s, 1H, quinoline-H4), 7.84 (d, $J=9.2$ Hz, 1H, quinoline-H8), 7.46 (d, $J=8.8$, 2H, phenyl-H2, H6 protons), 7.41 (s, 1H, quinoline-H5), 7.38 (d, $J=9.2$ Hz, 1H, quinoline-H7), 6.54 (d, $J=8.8$ Hz, 2H, phenyl-H3, H5 protons), 6.48 (brs, 2H, NH₂, D₂O-exchangeable), 5.55 (brs, 2H, NH₂, D₂O-exchangeable), 5.35 (t, $J=10.4$ Hz, 1H, pyrazole-H5), 3.88 (dd, $J=11.2$ Hz, $J=16.8$ Hz, 1H, pyrazole-H4 axial proton), 3.84 (s, 3H, quinoline OCH₃), 3.14 (dd, $J=10$ Hz, $J=12$ Hz, 1H, pyrazole-H4 equatorial proton); ¹³C NMR (DMSO-*d*₆) δ : 165.9, 159.4, 153.4, 151.0, 147.9, 142.7, 139.2, 137.1, 129.4, 128.4, 127.7, 126.7, 121.8, 116.3, 106.5, 64.2, 55.5, 37.1; MS (*m/z*) 397 (5.3%, M⁺+2), 395 (16.7%, M⁺), 203 (27%), 192 (100%); Anal. Calc. for: (C₂₀H₁₈ClN₅O₂): C, 60.69; H, 4.58; N, 17.69%; Found: C, 60.76; H, 4.63; N, 17.74%.

4.1.2.11. 5-(2-Chloro-6-methoxyquinolin-3-yl)-3-(3,4,5-trimethoxyphenyl)-4,5-dihydro-1H-pyrazole-1-carboxamide (19). Yellow solid (63%) mp = 117–118 °C; IR (KBr) cm⁻¹: 3317, 3290 (NH₂), 3031 (CH aromatic), 2934 (CH aliphatic), 1678 (C=O); ¹H NMR (DMSO-*d*₆) δ : 8.37 (s, 1H, quinoline-H4), 7.83 (d, $J=9.3$ Hz, 1H, quinoline-H8), 7.77 (s, 2H, phenyl-H2, H6 protons), 7.52 (d, $J=9.3$ Hz, 1H, quinoline-H7), 7.37 (s, 1H, quinoline-H5), 6.52 (brs, 2H, NH₂, D₂O-exchangeable), 5.14 (t, $J=6.6$ Hz, 1H, pyrazole-H5), 3.91 (s, 6H, 2OCH₃), 3.83 (s, 6H, 2OCH₃), 3.72 (dd, $J=15.4$ Hz, $J=7.2$ Hz, 1H, pyrazole-H4 axial proton), 3.28 (dd, $J=13.5$ Hz, $J=7.5$ Hz, 1H, pyrazole-H4 equatorial proton); ¹³C NMR (DMSO-*d*₆) δ : 166.6, 157.9, 153.8, 152.7, 149.3, 144.4, 142.3, 136.8, 133.3, 127.7, 127.1, 126.0, 123.2, 115.6, 106.5, 63.8, 56.9, 54.5, 54.2, 36.8; MS (*m/z*) 472 (25%, M⁺+2), 470 (73%, M⁺), 192 (100%); Anal. Calc. for: (C₂₃H₂₃ClN₄O₅): C, 58.66; H, 4.92; N, 11.90%; Found: C, 58.69; H, 4.98; N, 11.94%.

4.1.2.12. 2-Chloro-3-[3-(4-chlorophenyl)-1-phenyl-4,5-dihydro-1H-pyrazol-5-yl]-6-methoxyquinoline (20). Yellow solid (69%) mp = 145–146 °C; IR (KBr) cm⁻¹: 3024 (CH aromatic), 2951 (CH aliphatic); ¹H NMR (DMSO-*d*₆) δ : 8.57 (s, 1H, quinoline-H4), 8.41 (d, $J=8.4$ Hz, 2H, chlorophenyl-H2, H6 protons), 8.10–7.94 (m, 4H, quinoline-H5, H8 and phenyl-H2, H6), 7.80 (d, $J=8$ Hz, 2H, chlorophenyl-H3, H5 protons), 7.58 (t, $J=5.6$, 1H, phenyl-H4), 7.27 (d, $J=7.6$ Hz, 1H, quinoline-H7), 6.99 (d, $J=5.6$ Hz, 2H, phenyl-H3, H5), 5.78 (t, $J=6.8$, 1H, pyrazole-H5), 3.83 (dd, $J=4.4$, $J=10$, 1H, pyrazole-H4 axial proton), 3.76 (s, 3H, quinoline OCH₃), 2.68 (dd, $J=7.2$, $J=9.2$, 1H, pyrazole-H4 equatorial proton); ¹³C NMR (DMSO-*d*₆) δ : 159.4, 158.3, 153.6, 147.5, 134.2, 133.2, 132.3, 130.5, 129.5, 129.4, 129.3, 129.2, 128.2, 126.1, 123.8, 106.6, 57.6, 55.9, 36.9; MS (*m/z*) 452 (1.1%, M+4), 450 (6.7%, M+2), 448 (9.6%, M⁺), 255 (100%); Anal. Calc. for: (C₂₅H₁₉Cl₂N₃O): C, 66.97; H, 4.27; N, 9.37%; Found: C, 67.07; H, 4.34; N, 9.42%.

4.1.2.13. 4-[5-(2-Chloro-6-methoxyquinolin-3-yl)-1-phenyl-4,5-dihydro-1H-pyrazol-3-yl]aniline (21). Orange solid (55%) mp = 136–137 °C; IR (KBr) cm⁻¹: 3315, 3297 (NH₂), 3066 (CH aromatic), 2968 (CH aliphatic); ¹H NMR (DMSO-*d*₆) δ : 8.41 (s, 1H, quinoline-H4), 7.85 (d, $J=9.2$ Hz, 1H, quinoline-H8), 7.54 (s, 1H, quinoline-H5), 7.44–7.37 (m, 3H, quinoline-H7 and aminophenyl-H2, H6 protons), 7.19–7.12 (m, 3H, phenyl-H3, H5 and H4), 6.90 (d, $J=8$, 2H, aminophenyl-H3, H5 protons), 6.57 (d, $J=8.4$ Hz, 2H,

phenyl-H3, H5), 5.47 (brs, 2H, NH₂, D₂O-exchangeable), 5.16 (t, $J=8$ Hz, 1H, pyrazole-H5), 3.77 (s, 3H, quinoline OCH₃), 3.65 (dd, $J=9.2$ Hz, $J=16.8$ Hz, 1H, pyrazole-H4 axial proton), 3.17 (dd, $J=10.4$ Hz, $J=16.4$ Hz, 1H, pyrazole-H4 equatorial proton); ¹³C NMR (DMSO-*d*₆) δ : 160.1, 153.4, 150.3, 148.3, 142.7, 139.5, 137.8, 134.3, 132.3, 129.1, 128.4, 127.4, 126.7, 122.9, 121.8, 116.6, 105.9, 59.0, 55.2, 37.5; MS (*m/z*) 430 (9.3%, M⁺ +2), 428 (27.9%, M⁺), 236 (47%), 192 (100%); Anal. Calc. for: (C₂₅H₂₁ClN₄O): C, 70.01; H, 4.94; N, 13.06%; Found: C, 70.08; H, 4.99; N, 13.12%.

4.1.2.14. 2-Chloro-6-methoxy-3-[1-phenyl-3-(3,4,5-trimethoxyphenyl)-4,5-dihydro-1H-pyrazol-5-yl]quinoline (22). Brown solid (58%) mp = 136–137 °C; IR (KBr) cm⁻¹: 3024 (CH aromatic), 2941 (CH aliphatic); ¹H NMR (DMSO-*d*₆) δ : 8.46 (s, 1H, quinoline-H4), 8.00 (d, $J=9.2$ Hz, 1H, quinoline-H8), 7.88 (d, $J=9.6$ Hz, 1H, quinoline-H7), 7.73 (d, $J=8$ Hz, 2H, methoxyphenyl-H2, H6 protons), 7.58–7.46 (m, 6H, aromatic protons), 5.14 (t, $J=9.2$ Hz, 1H, pyrazole-H5), 3.87 (s, 6H, 2OCH₃), 3.76 (s, 6H, 2OCH₃), 3.66 (dd, $J=5.2$ Hz, $J=11$ Hz, 1H, pyrazole-H4 axial proton), 2.86 (dd, $J=11.2$ Hz, $J=15.2$ Hz, 1H, 1H, pyrazole-H4 equatorial proton); ¹³C NMR (DMSO-*d*₆) δ : 159.3, 157.9, 154.2, 153.4, 150.3, 149.3, 144.4, 142.4, 136.8, 133.3, 130.1, 129.1, 128.1, 127.4, 126.4, 123.6, 115.9, 106.2, 61.8, 56.9, 55.5, 37.8; MS (*m/z*) 505 (22%, M + 2), 503 (68%, M⁺), 311 (100%); Anal. Calc. for: (C₂₈H₂₆ClN₃O₄): C, 66.73; H, 5.20; N, 8.34%; Found: C, 66.79; H, 5.25; N, 8.38%.

4.1.2.15. 2-Chloro-3-[3-(4-chlorophenyl)-1-(2,4-dinitrophenyl)-4,5-dihydro-1H-pyrazol-5-yl]-6-methoxyquinoline (23). Yellow solid (63%) mp = 143–144 °C; IR (KBr) cm⁻¹: 3047 (CH aromatic), 2973 (CH aliphatic); ¹H NMR (DMSO-*d*₆) δ : 9.54 (s, 1H, nitrophenyl-H3), 8.74 (d, $J=4.4$ Hz, 1H, nitrophenyl-H5), 8.69 (d, $J=4.4$ Hz, 1H, 1H, nitrophenyl-H6), 8.61 (s, 1H, quinoline-H4), 8.10 (d, $J=6.8$ Hz, 2H, chlorophenyl-H2, H6 protons), 8.20 (s, 1H, quinoline-H5), 7.95 (d, $J=5.2$ Hz, 1H, quinoline-H8), 7.76 (d, $J=5.6$ Hz, 1H, quinoline-H7), 7.56 (d, $J=5.2$ Hz, 2H, chlorophenyl-H3, H5 protons), 4.61 (t, $J=10$, 1H, pyrazole-H5), 3.74 (s, 3H, quinoline OCH₃), 3.59 (dd, $J=9.2$, $J=16.4$, 1H, pyrazole-H4 axial proton), 2.78 (dd, $J=12$, $J=17.2$, 1H, pyrazole-H4 equatorial proton); ¹³C NMR (DMSO-*d*₆) δ : 153.4, 150.3, 146.8, 144.7, 141.2, 137.8, 136.4, 134.3, 133.3, 130.8, 130.1, 129.4, 128.4, 128.2, 127.4, 126.4, 125.6, 123.9, 106.5, 56.9, 55.9, 37.1; MS (*m/z*) 542 (2.7%, M⁺ +4), 540 (16%, M + 2), 538 (24.6%, M⁺), 345 (100%); Anal. Calc. for: (C₂₅H₁₇Cl₂N₅O₅): C, 55.78; H, 3.18; N, 13.01%; Found: C, 55.85; H, 3.24; N, 13.08%.

4.1.2.16. 4-[5-(2-Chloro-6-methoxyquinolin-3-yl)-1-(2,4-dinitrophenyl)-4,5-dihydro-1H-pyrazol-3-yl]aniline (24). Yellow solid (57%) mp = 139–140 °C; IR (KBr) cm⁻¹: 3300, 3292 (NH₂), 3021 (CH aromatic), 2923 (CH aliphatic); ¹H NMR (DMSO-*d*₆) δ : 8.85 (s, 1H, nitrophenyl-H3), 8.83 (d, $J=2.8$ Hz, 1H, nitrophenyl-H5), 8.41 (s, 1H, quinoline-H4), 8.29 (d, $J=2.8$ Hz, 1H, nitrophenyl-H6), 8.0 (d, $J=9.2$ Hz, 1H, quinoline-H8), 7.77 (d, $J=9.2$, 1H, quinoline-H7), 7.47 (s, 1H, quinoline-H5), 7.40 (d, $J=8.8$ Hz, 2H, aminophenyl-H2, H6), 6.84 (d, $J=8.8$ Hz, 2H, aminophenyl-H3, H5), 5.36 (brs, 2H, NH₂, D₂O-exchangeable), 4.98 (t, $J=6$ Hz, 1H, pyrazole-H5), 3.88 (s, 3H, quinoline OCH₃), 3.70 (dd, $J=10$ Hz, $J=14.4$ Hz, 1H, pyrazole-H4 axial proton), 2.82 (dd, $J=9.6$ Hz, $J=17.2$ Hz, 1H, pyrazole-H4 equatorial proton); ¹³C NMR (DMSO-*d*₆) δ : 162.4, 157.6, 156.9, 153.5, 150.6, 149.3, 145.8, 142.4, 139.2, 137.5, 133.3, 131.9, 129.1, 128.4, 127.7, 127.1, 123.9, 121.5, 116.3, 106.9, 57.2, 55.5, 37.5; MS (*m/z*) 520 (9.3%, M + 2), 518 (27.9%, M⁺), 326 (38%), 192 (100%); Anal. Calc. for: (C₂₅H₁₉ClN₆O₅): C, 57.87; H, 3.69; N, 16.20%; Found: C, 57.93; H, 3.74; N, 16.26%.

4.1.2.17. 2-Chloro-3-[1-(2,4-dinitrophenyl)-3-(3,4,5-trimethoxyphenyl)-4,5-dihydro-1H-pyrazol-5-yl]-6-methoxyquinoline (25). Orange solid (61%) mp = 135–136 °C; IR (KBr) cm⁻¹: 3039 (CH aromatic), 2922 (CH aliphatic); ¹H NMR (DMSO-*d*₆) δ : 9.03 (s, 1H, nitrophenyl-H3), 8.94 (d, $J=5.7$ Hz, 1H, nitrophenyl-H5), 8.43 (s, 1H, quinoline-H4), 7.97 (d, $J=9.3$ Hz, 1H, quinoline-H8), 7.52 (s, 2H, methoxyphenyl-H2, H6), 7.50 (d, $J=9.3$ Hz, 1H, quinoline-H7), 7.42 (s, 1H, quinoline-H5), 7.34 (d, $J=5.7$ Hz, 1H, 1H, nitrophenyl-H6), 5.30 (t, $J=5.4$ Hz, 1H, pyrazole-H5), 3.94 (s, 6H, 2OCH₃), 3.91 (s, 6H, 2OCH₃), 3.71 (dd, $J=7.2$ Hz, $J=14.4$ Hz, 1H, pyrazole-H4 axial proton), 2.52 (dd, $J=6.3$ Hz, $J=12.3$ Hz, 1H, pyrazole-H4 equatorial proton); ¹³C NMR (DMSO-*d*₆) δ : 157.9, 156.2, 155.5, 153.8, 153.1, 149.3, 144.7, 142.7, 136.8, 134.0, 133.3, 129.4, 129.1, 127.7, 127.4, 126.0, 123.6, 119.4, 115.6, 106.5, 56.9, 55.5, 51.3, 37.1; MS (*m/z*) 595 (9%, M⁺ +2), 593 (28%, M⁺), 401 (100%); Anal. Calc. for: (C₂₈H₂₄ClN₅O₈): C, 56.62; H, 4.07; N, 11.79%; Found: C, 56.65; H, 4.10; N, 11.84%.

4.1.3. General procedure for synthesis of compounds (26–31)

A mixture of chalcone **5–7** (10 mmole) and thiourea or guanidine hydrochloride (10 mmole) was stirred in absolute ethanol (20 mL), and then sodium hydroxide (0.8 g, 20 mmole) was added. The reaction mixture was heated under reflux for 8 h. After completion of reaction, as detected by TLC, the solvent was concentrated under reduced pressure, and then poured into ice water (50 mL). The obtained solid was filtered off, washed and recrystallized from ethanol to afford the desired compounds **26–31**.

4.1.3.1. 6-(2-Chloro-6-methoxyquinolin-3-yl)-4-(4-chlorophenyl)pyrimidine-2(1H)-thione (26). Yellow solid (54%) mp = 155–156 °C; IR (KBr) cm⁻¹: 3308 (NH), 3056 (CH aromatic), 2969 (CH aliphatic); ¹H NMR (DMSO-*d*₆) δ : 14.16 (brs, 1H, NH, D₂O-exchangeable), 8.61 (s, 1H, quinoline-H4), 8.34 (d, $J=8.8$ Hz, 1H, quinoline-H8), 8.14 (d, $J=8.4$ Hz, 2H, phenyl-H2, H6 protons), 7.86 (d, $J=8.8$ Hz, 1H, quinoline-H7), 7.55 (d, $J=8.4$ Hz, 2H, phenyl-H3, H5 protons), 7.42 (s, 1H, pyrimidine-H5), 7.33 (s, 1H, quinoline-H5), 3.81 (s, 3H, quinoline OCH₃); ¹³C NMR (DMSO-*d*₆) δ : 166.6, 160.1, 159.0, 157.9, 153.8, 147.5, 144.7, 142.3, 134.3, 133.3, 130.5, 129.1, 128.4, 128.1, 126.4, 123.9, 106.2, 55.9; MS (*m/z*) 418 (2.4%, M + 4), 416 (15.4%, M + 2), 414 (22.5%, M⁺), 220 (33%), 192 (100%); Anal. Calc. for: (C₂₀H₁₃Cl₂N₃O₅): C, 57.98; H, 3.16; N, 10.14%; Found: C, 58.04; H, 3.22; N, 10.19%.

4.1.3.2. 4-(4-Aminophenyl)-6-(2-chloro-6-methoxyquinolin-3-yl)pyrimidine-2(1H)-thione (27). Yellow solid (63%) mp = 146–147 °C; IR (KBr) cm⁻¹: 3311, 3299 (NH₂), 3039 (CH aromatic), 2974 (CH aliphatic); ¹H NMR (DMSO-*d*₆) δ : 12.74 (brs, 1H, NH, D₂O-exchangeable), 8.09 (s, 1H, quinoline-H4), 7.86 (d, $J=8.8$ Hz, 1H, quinoline-H8), 7.45 (d, $J=8.8$ Hz, 1H, quinoline-H7), 7.41 (s, 1H, pyrimidine-H5), 7.15 (d, $J=8.4$ Hz, 2H, phenyl-H2, H6 protons), 6.49 (d, $J=8.4$ Hz, 2H, phenyl-H2, H6 protons), 6.41 (s, 1H, quinoline-H5), 5.32 (brs, 2H, NH₂, D₂O-exchangeable), 3.88 (s, 3H, quinoline OCH₃); ¹³C NMR (DMSO-*d*₆) δ : 165.9, 159.7, 159.0, 157.6, 153.4, 148.3, 142.7, 139.5, 131.6, 129.5, 128.1, 127.4, 126.7, 123.2, 121.2, 116.3, 106.2, 55.5; MS (*m/z*) 396 (5.4%, M⁺ +2), 394 (16.6%, M⁺), 202 (39%), 302 (100%); Anal. Calc. for: (C₂₀H₁₅ClN₄O₅): C, 60.83; H, 3.83; N, 14.19%; Found: C, 60.87; H, 3.88; N, 14.22%.

4.1.3.3. 6-(2-Chloro-6-methoxyquinolin-3-yl)-4-(3,4,5-trimethoxyphenyl)pyrimidine-2(1H)-thione (28). Yellow solid (54%)

mp = 141–142 °C; IR (KBr) cm^{-1} : 3275 (NH), 3028 (CH aromatic), 2932 (CH aliphatic); ^1H NMR (DMSO- d_6) δ : 10.83 (brs, 1H, NH, D₂O-exchangeable), 8.75 (s, 1H, quinoline-H4), 7.83 (d, J = 9.3 Hz, 1H, quinoline-H8), 7.52 (d, J = 9.3 Hz, 1H, quinoline-H7), 7.37 (s, 1H, pyrimidine-H5), 7.18 (s, 2H, phenyl-H2, H6 protons), 7.07 (s, 1H, quinoline-H5), 3.94 (s, 6H, 2OCH₃), 3.89 (s, 6H, 2OCH₃); ^{13}C NMR (DMSO- d_6) δ : 166.6, 163.8, 159.1, 153.8, 152.8, 148.9, 144.7, 142.7, 136.8, 134.3, 133.6, 128.4, 127.7, 126.4, 123.6, 115.6, 106.5, 56.5, 54.8, 54.4; MS (m/z) 471 (3%, M⁺ + 2), 469 (10%, M⁺), 70 (100%); Anal. Calc. for: (C₂₃H₂₀ClN₃O₄S): C, 58.78; H, 4.29; N, 8.94%; Found: C, 58.79; H, 4.33; N, 8.99%.

4.1.3.4. 4-(2-Chloro-6-methoxyquinolin-3-yl)-6-(4-chlorophenyl)pyrimidin-2-amine (29). Yellow solid (72%) mp = 195–196 °C; IR (KBr) cm^{-1} : 3321, 3284 (NH₂), 3049 (CH aromatic), 2972 (CH aliphatic); ^1H NMR (DMSO- d_6) δ : 8.49 (s, 1H, quinoline-H4), 8.37 (d, J = 8.8 Hz, 1H, quinoline-H8), 7.79 (d, J = 8.4 Hz, 2H, phenyl-H2, H6 protons), 7.50 (s, 1H, pyrimidine-H5), 7.11 (s, 1H, quinoline-H5), 7.05 (d, J = 8.4 Hz, 2H, phenyl-H3, H5 protons), 6.78 (d, J = 8.8 Hz, 1H, quinoline-H7), 5.41 (brs, 2H, NH₂, D₂O-exchangeable), 3.72 (s, 3H, quinoline OCH₃); ^{13}C NMR (DMSO- d_6) δ : 162.8, 160.1, 159.4, 157.9, 153.8, 146.5, 144.4, 142.7, 134.0, 132.6, 130.5, 129.1, 128.1, 127.4, 126.0, 123.6, 106.5, 55.5; MS (m/z) 376 (1.4%, M + 4), 374 (7.4%, M⁺ + 2), 372 (11%, M⁺), 204 (33%), 192 (100%); Anal. Calc. for: (C₂₀H₁₄Cl₂N₄O): C, 60.47; H, 3.55; N, 14.10%; Found: C, 60.54; H, 3.61; N, 14.17%.

4.1.3.5. 4-(4-Aminophenyl)-6-(2-chloro-6-methoxyquinolin-3-yl)pyrimidin-2-amine (30). Yellow solid (58%) mp = 175–176 °C; IR (KBr) cm^{-1} : 3327, 3289 (NH₂), 3028 (CH aromatic), 2918 (CH aliphatic); ^1H NMR (DMSO- d_6) δ : 8.51 (s, 1H, quinoline-H4), 8.13 (s, 1H, pyrimidine-H5), 7.84 (d, J = 8.4 Hz, 1H, quinoline-H7), 7.62 (d, J = 8.8 Hz, 2H, phenyl-H2, H6 protons), 7.43 (d, J = 8.4 Hz, 1H, quinoline-H8), 7.25 (s, 1H, quinoline-H5), 6.82 (d, J = 8.8 Hz, 2H, phenyl-H3, H5 protons), 5.50 (brs, 2H, NH₂, D₂O-exchangeable), 5.30 (brs, 2H, NH₂, D₂O-exchangeable), 3.71 (s, 3H, quinoline OCH₃); ^{13}C NMR (DMSO- d_6) δ : 164.2, 162.4, 159.4, 157.6, 153.8, 148.9, 142.3, 139.9, 132.3, 129.4, 128.4, 127.7, 126.7, 121.5, 119.0, 116.6, 105.9, 55.2; MS (m/z) 379 (11.4%, M⁺ + 2), 377 (35.6%, M⁺), 185 (66%), 302 (100%); Anal. Calc. for: (C₂₀H₁₆ClN₅O): C, 63.58; H, 4.27; N, 18.54%; Found: C, 63.66; H, 4.33; N, 18.59%.

4.1.3.6. 4-(2-Chloro-6-methoxyquinolin-3-yl)-6-(3,4,5-trimethoxyphenyl)pyrimidin-2-amine (31). brown solid (69%) mp = 162–163 °C; IR (KBr) cm^{-1} : 3303, 3291 (NH₂), 3024 (CH aromatic), 2949 (CH aliphatic); ^1H NMR (DMSO- d_6) δ : 8.53 (s, 1H, quinoline-H4), 7.95 (d, J = 9 Hz, 1H, quinoline-H8), 7.54 (s, 1H, pyrimidine-H5), 7.51 (d, J = 9 Hz, 1H, quinoline-H7), 7.42 (s, 1H, quinoline-H5), 7.25 (s, 2H, phenyl-H2, H6 protons), 6.8 (brs, 2H, NH₂, D₂O-exchangeable), 3.91 (s, 6H, 2OCH₃), 3.83 (s, 6H, 2OCH₃); ^{13}C NMR (DMSO- d_6) δ : 168.3, 162.1, 159.4, 153.8, 153.5, 149.6, 144.7, 142.4, 136.7, 134.0, 133.0, 128.1, 127.4, 126.4, 123.6, 115.3, 106.2, 56.9, 55.2, 54.8; MS (m/z) 454 (0.6%, M + 2), 452 (2%, M⁺), 192 (100%); Anal. Calc. for: (C₂₃H₂₁ClN₄O₄): C, 61.00; H, 4.67; N, 12.37%; Found: C, 61.07; H, 4.70; N, 12.44%.

4.1.4. General procedure for synthesis of compounds (32–34)

A mixture of chalcone **5–7** (10 mmole) and urea (0.6 g, 10 mmole) was stirred in ethanol (20 mL), and then hydrochloric acid (2 mL) was added. The mixture was heated at reflux for 12 h. After completion the reaction, the solvent was concentrated under reduced

pressure and poured into ice water (50 mL). The obtained precipitate was filtered off, washed and recrystallized from ethanol to yield the titled compounds **32–34**.

4.1.4.1. 6-(2-Chloro-6-methoxyquinolin-3-yl)-4-(4-chlorophenyl)pyrimidin-2(1H)-one (32). Yellow solid (76%) mp = 180–181 °C; IR (KBr) cm^{-1} : 3332 (NH), 3078 (CH aromatic), 2932 (CH aliphatic); ^1H NMR (DMSO- d_6) δ : 11.96 (brs, 1H, NH, D₂O-exchangeable), 8.51 (s, 1H, quinoline-H4), 8.33 (d, J = 8.2 Hz, 1H, quinoline-H8), 8.06 (d, J = 8.8 Hz, 2H, phenyl-H2, H6 protons), 7.77 (d, J = 8.2 Hz, 1H, quinoline-H7), 7.28 (s, 1H, pyrimidine-H5), 7.20 (s, 1H, quinoline-H5), 7.08 (d, J = 8.8 Hz, 2H, phenyl-H3, H5 protons), 3.74 (s, 3H, quinoline OCH₃); ^{13}C NMR (DMSO- d_6) δ : 166.3, 160.1, 159.0, 157.9, 153.8, 147.5, 144.7, 142.7, 134.3, 133.6, 130.5, 129.8, 128.1, 127.1, 126.0, 123.6, 105.5, 55.2; MS (m/z) 402 (1.4%, M⁺ + 4), 400 (9%, M + 2), 398 (13%, M⁺), 204 (33%), 192 (100%); Anal. Calc. for: (C₂₀H₁₃Cl₂N₃O₂): C, 60.32; H, 3.29; N, 10.55%; Found: C, 60.40; H, 3.35; N, 10.61%.

4.1.4.2. 4-(4-Aminophenyl)-6-(2-chloro-6-methoxyquinolin-3-yl)pyrimidin-2(1H)-one (33). Yellow solid (76%) mp = 171–172 °C; IR (KBr) cm^{-1} : 3322, 3285 (NH₂), 3023 (CH aromatic), 2917 (CH aliphatic); ^1H NMR (DMSO- d_6) δ : 10.41 (brs, 1H, NH, D₂O-exchangeable), 8.12 (s, 1H, quinoline-H4), 7.84 (d, J = 8.8 Hz, 2H, phenyl-H2, H6 protons), 7.59 (d, J = 8.4 Hz, 1H, quinoline-H8), 7.30 (d, J = 8.4 Hz, 1H, quinoline-H7), 7.20 (s, 1H, pyrimidine-H5), 6.62 (d, J = 8.8 Hz, 2H, phenyl-H3, H5 protons), 6.15 (s, 1H, quinoline-H5), 5.32 (brs, 2H, NH₂, D₂O-exchangeable), 3.79 (s, 3H, quinoline OCH₃); ^{13}C NMR (DMSO- d_6) δ : 169.8, 160.1, 159.0, 157.6, 153.8, 148.9, 142.4, 139.5, 131.9, 129.1, 128.4, 127.7, 127.1, 124.2, 121.8, 116.3, 105.9, 55.2; MS (m/z) 380 (9.1%, M + 2), 378 (28.6%, M⁺), 92 (25%), 286 (100%); Anal. Calc. for: (C₂₀H₁₅ClN₄O₂): C, 63.41; H, 3.99; N, 14.79%; Found: C, 63.44; H, 4.02; N, 14.83%.

4.1.4.3. 6-(2-Chloro-6-methoxyquinolin-3-yl)-4-(3,4,5-trimethoxyphenyl)pyrimidin-2(1H)-one (34). Yellow solid (74%) mp = 176–177 °C; IR (KBr) cm^{-1} : 3319 (NH), 3055 (CH aromatic), 2912 (CH aliphatic); ^1H NMR (DMSO- d_6) δ : 11.96 (brs, 1H, NH, D₂O-exchangeable), 8.52 (s, 1H, quinoline-H4), 8.35 (d, J = 9 Hz, 1H, quinoline-H8), 7.79 (d, J = 9 Hz, 1H, quinoline-H7), 7.32 (s, 1H, pyrimidine-H5), 7.24 (s, 2H, phenyl-H2, H6 protons), 7.13 (s, 1H, quinoline-H5), 3.88 (s, 6H, 2OCH₃), 3.82 (s, 6H, 2OCH₃); ^{13}C NMR (DMSO- d_6) δ : 162.4, 161.1, 159.4, 153.5, 153.1, 148.9, 144.7, 142.3, 136.8, 134.3, 137.3, 128.4, 128.1, 126.7, 123.9, 115.9, 106.5, 56.9, 55.2, 54.8; MS (m/z) 455 (1.6%, M⁺ + 2), 453 (6%, M⁺), 167 (100%); Anal. Calc. for: (C₂₃H₂₀ClN₃O₅): C, 60.86; H, 4.44; N, 9.26%; Found: C, 60.92; H, 4.50; N, 9.29%.

4.2. Biological evaluation

4.2.1. In vitro cytotoxic activity

Evaluation of cytotoxic activity of the synthesised compounds was carried out using MTT assay protocol^{46–48} against a group of cancer cell lines namely; colorectal carcinoma (HCT-116), Hepatocellular carcinoma (HepG-2) and breast cancer (MCF-7) and colchicine was used as a standard drug. The complete procedure was depicted in Supplementary data.

4.2.2. In vitro tubulin polymerisation assay

The effect of the synthesised compounds on tubulin polymerisation was assessed turbidimetrically using a fluorescent plate

reader method⁴⁹. The complete procedure was depicted in [Supplementary data](#).

4.2.3. Cell cycle analysis

The effect of the most promising compound **25** on cell cycle was evaluated using flowcytometer^{50,53,54} as illustrated in [Supplementary data](#).

4.2.4. Annexin V-FITC apoptosis assay

The effect of compound **25** on apoptosis induction was analysed using Annexin V-FITC/PI apoptosis detection kit using flowcytometer^{51,55,56} as illustrated in [Supplementary data](#).

4.3. Docking studies

The Crystal structure of the target receptor (tubulin) [PDB ID: 1SA0, resolution 3.00 Å] was obtained from Protein Data Bank (<http://www.pdb.org>). The docking process was carried out using MOE2014 software. At first, the crystal structure of the target was prepared by removing water molecules and retaining the two essential chains and the co-crystallised ligand, *N*-deacetyl-*N*-(2-mercaptoacetyl)-colchicine (DAMA-colchicine). Then, the protein structure was protonated, and the hydrogen atoms were hidden. Next, the energy was minimised, and the binding pocket of the protein was defined.

The 2D structures of the synthesised compounds and reference ligand (DAMA-colchicine) were sketched using ChemBioDraw Ultra 14.0 and saved as MDL-SD format⁵⁷. Then, the saved files were opened using MOE and 3D structures were protonated. Next, energy minimisation was applied. Before docking process, validation of the docking protocol was carried out by running the simulation only using the co-crystallised ligand (DAMA-colchicine) which showed low RMSD value. The molecular docking of the synthesised was performed using a default protocol against the target receptor. In each case, 30 docked structures were generated using genetic algorithm searches, London dG was used for scoring and forcefield (MMFF94) for refinement. The London dG scoring function estimates the free energy of binding of the ligand from a given pose. The output from MOE was further analysed and visualised using Discovery Studio 4.0 software.^{58–63}

Disclosure statement

No potential conflict of interest was reported by the author(s).

References

- Weinberg RA. How cancer arises. *Sci Am* 1996;275:62–70.
- Johnson DS, Li JJ. The art of drug synthesis. Hoboken: John Wiley & Sons; 2013.
- N.C. Institute, Cancer Statistics. 2019. Available from: <https://www.cancer.gov/about-cancer/understanding/statistics> [last accessed May 2019].
- Miller KD, Siegel RL, Lin CC, et al. Cancer treatment and survivorship statistics, 2016. *CA: Cancer J Clin* 2016;66:271–89.
- Chau M-F, Radeke MJ, de Inés C, et al. The microtubule-associated protein tau cross-links to two distinct sites on each alpha and beta tubulin monomer via separate domains. *Biochemistry* 1998;37:17692–703.
- Field JJ, Kanakkanthara A, Miller JH. Microtubule-targeting agents are clinically successful due to both mitotic and interphase impairment of microtubule function. *Bioorg Med Chem* 2014;22:5050–9.
- Kavallaris M. Microtubules and resistance to tubulin-binding agents. *Nat Rev Cancer* 2010;10:194–204.
- Giannakakou P, Sackett D, Fojo T. Tubulin/microtubules: still a promising target for new chemotherapeutic agents. *J Natl Cancer Inst* 2000;92:182–3.
- Wilson L, Jordan MA. Microtubule dynamics: taking aim at a moving target. *Chem Biol* 1995;2:569–73.
- Jordan MA, Wilson L. Microtubules as a target for anticancer drugs. *Nat Rev Cancer* 2004;4:253–65.
- Botta M, Forli S, Magnani M, Manetti F. Molecular modeling approaches to study the binding mode on tubulin of microtubule destabilizing and stabilizing agents. *Tubulin-Binding Agents*. Berlin: Springer; 2008:279–328.
- Altaha R, Fojo T, Reed E, Abraham J. Epothilones: a novel class of non-taxane microtubule-stabilizing agents. *Curr Pharm Des* 2002;8:1707–12.
- Prota AE, Bargsten K, Diaz JF, et al. A new tubulin-binding site and pharmacophore for microtubule-destabilizing anticancer drugs. *Proc Natl Acad Sci USA* 2014;111:13817–21.
- Lu Y, Chen J, Xiao M, et al. An overview of tubulin inhibitors that interact with the colchicine binding site. *Pharm Res* 2012;29:2943–71.
- Li L, Jiang S, Li X, et al. Recent advances in trimethoxyphenyl (TMP) based tubulin inhibitors targeting the colchicine binding site. *Eur J Med Chem* 2018;151:482–94.
- Zhou J, Giannakakou P. Targeting microtubules for cancer chemotherapy. *Curr Med Chem Anticancer Agents* 2005;5:65–71.
- Pettit GR, Lippert JW, Herald DL, et al. Antineoplastic agents 440. Asymmetric synthesis and evaluation of the combretastatin A-1 SAR Probes (1S,2S)- and (1R,2R)-1, 2-dihydroxy-1-(2',3'-dihydroxy-4'-methoxyphenyl)-2-(3'',4'',5''-trimethoxyphenyl)-ethane. *J. Nat. Prod* 2000;63:969–74.
- Pettit GR, Lippert JW. Antineoplastic agents 429. Syntheses of the combretastatin A-1 and combretastatin B-1 prodrugs. *Anticancer Drug Design* 2000;15:203–16.
- Pettit GR, Temple JC, Narayanan V, et al. Antineoplastic agents 322. synthesis of combretastatin A-4 prodrugs. *Anti-Cancer Drug Des* 1995;10:299–309.
- Kirwan IG, Loadman PM, Swaine DJ, et al. Comparative pre-clinical pharmacokinetic and metabolic studies of the combretastatin prodrugs combretastatin A4 phosphate and A1 phosphate. *Clin Cancer Res* 2004;10:1446–53.
- Ding Z, Cheng H, Wang S, et al. Development of MBRI-001, a deuterium-substituted plinabulin derivative as a potent anti-cancer agent. *Bioorg Med Chem Lett* 2017;27:1416–9.
- Lloyd GK, Mueller P, Zippelius A, Huang L. Abstract A07: plinabulin: evidence for an immune-mediated mechanism of action. *AACR* 2016;76:A07–A07.
- Plinabulin accepted for the prevention of neutropenia. *Oncology Times* 2017;39:25.
- Kapoor S, Srivastava S, Panda D. Indibulin dampens microtubule dynamics and produces synergistic antiproliferative effect with vinblastine in MCF-7 cells: implications in cancer chemotherapy. *Sci Rep* 2018;8:12363.
- Bacher G, Nickel B, Emig P, et al. D-24851, a novel synthetic microtubule inhibitor, exerts curative antitumoral activity *in vivo*, shows efficacy toward multidrug-resistant tumor cells, and lacks neurotoxicity. *Cancer Res* 2001;61:392–9.
- Hande KR, Hagey A, Berlin J, et al. The pharmacokinetics and safety of ABT-751, a novel, orally bioavailable

- sulfonamide antimetabolic agent: results of a phase 1 study. *Clin Cancer Res* 2006;12:2834–40.
27. Imbert T. Discovery of podophyllotoxins. *Biochimie* 1998;80:207–22.
 28. Liu YQ, Tian J, Qian K, et al. Recent progress on C-4-modified podophyllotoxin analogs as potent antitumor agents. *Med Res Rev* 2015;35:1–62.
 29. Lee L, Davis R, Vanderham J, et al. 1, 2, 3, 4-Tetrahydro-2-thioxopyrimidine analogs of combretastatin-A4. *Eur J Med Chem* 2008;43:2011–5.
 30. Johnson M, Younglove B, Lee L, et al. Design, synthesis, and biological testing of pyrazoline derivatives of combretastatin-A4. *Bioorg Med Chem Lett* 2007;17:5897–901.
 31. Simoni D, Grisolia G, Giannini G, et al. Heterocyclic and phenyl double-bond-locked combretastatin analogues possessing potent apoptosis-inducing activity in HL60 and in MDR cell lines. *J. Med. Chem* 2005;48:723–36.
 32. Chamberlain MC, Grimm S, Phuphanich S, et al. A phase 2 trial of verubulin for recurrent glioblastoma: a prospective study by the Brain Tumor Investigational Consortium (BTIC). *J Neuro-Oncol* 2014;118:335–43.
 33. El-Zahabi MA, Sakr H, El-Adl K, et al. Design, synthesis, and biological evaluation of new challenging thalidomide analogs as potential anticancer immunomodulatory agents. *Bioorg Chem* 2020;104:104218.
 34. Nasser AA, Eissa IH, Oun MR, et al. Discovery of new pyrimidine-5-carbonitrile derivatives as anticancer agents targeting EGFRWT and EGFR790M. *Org Biomol Chem* 2020;18:7608–34.
 35. Abbass EM, Khalil AK, Mohamed MM, et al. Design, efficient synthesis, docking studies, and anticancer evaluation of new quinoxalines as potential intercalative Topo II inhibitors and apoptosis inducers. *Bioorg Chem* 2020;104:104255.
 36. El-Helby A-GA, Sakr H, Ayyad RR, et al. Design, synthesis, molecular modeling, in vivo studies and anticancer activity evaluation of new phthalazine derivatives as potential DNA intercalators and topoisomerase II inhibitors. *Bioorg Chem* 2020;103:104233.
 37. Mahdy HA, Ibrahim MK, Metwaly AM, et al. Design, synthesis, molecular modeling, in vivo studies and anticancer evaluation of quinazolin-4(3H)-one derivatives as potential VEGFR-2 inhibitors and apoptosis inducers. *Bioorg Chem* 2020;94:103422.
 38. El-Adl K, El-Helby A-GA, Sakr H, et al. Design, synthesis, molecular docking and anticancer evaluations of 5-benzylidenethiazolidine-2,4-dione derivatives targeting VEGFR-2 enzyme. *Bioorg Chem* 2020;102:104059.
 39. El-Naggar AM, Eissa IH, Belal A, El-Sayed AA. Design, eco-friendly synthesis, molecular modeling and anticancer evaluation of thiazol-5 (4H)-ones as potential tubulin polymerization inhibitors targeting the colchicine binding site. *RSC Adv* 2020;10:2791–811.
 40. El-Helby AGA, Sakr H, Eissa IH, et al. Benzoxazole/benzothiazole-derived VEGFR-2 inhibitors: design, synthesis, molecular docking, and anticancer evaluations. *Archiv der Pharmazie* 2019;352:1900178.
 41. Eissa IH, Metwaly AM, Belal A, et al. Discovery and antiproliferative evaluation of new quinoxalines as potential DNA intercalators and topoisomerase II inhibitors. *Archiv der Pharmazie* 2019;352:1900123.
 42. Elmetwally SA, Saied KF, Eissa IH, Elkaeed EB. Design, synthesis and anticancer evaluation of thieno[2,3-d]pyrimidine derivatives as dual EGFR/HER2 inhibitors and apoptosis inducers. *Bioorg Chem* 2019;88:102944.
 43. Tripathi A, Durrant D, Lee RM, et al. Hydrophobic analysis and biological evaluation of stilbene derivatives as colchicine site microtubule inhibitors with anti-leukemic activity. *J Enzyme Inhib Med Chem* 2009;24:1237–44.
 44. Nguyen TL, McGrath C, Hermone AR, et al. A common pharmacophore for a diverse set of colchicine site inhibitors using a structure-based approach. *J Med Chem* 2005;48:6107–16.
 45. Bhattacharyya B, Panda D, Gupta S, Banerjee M. Anti-mitotic activity of colchicine and the structural basis for its interaction with tubulin. *Med Res Rev* 2008;28:155–83.
 46. Mosmann T. Rapid colorimetric assay for cellular growth and survival: application to proliferation and cytotoxicity assays. *J Immunol Meth* 1983;65:55–63.
 47. Denizot F, Lang R. Rapid colorimetric assay for cell growth and survival. Modifications to the tetrazolium dye procedure giving improved sensitivity and reliability. *J Immunol Methods* 1986;89:271–7.
 48. Thabrew M, Hughes RD, Mcfarlane IG. Screening of hepatoprotective plant components using a HepG2 cell cytotoxicity assay. *J Pharm Pharmacol* 1997;49:1132–5.
 49. Morris GM, Goodsell DS, Halliday RS, et al. Automated docking using a Lamarckian genetic algorithm and an empirical binding free energy function. *J Comput Chem* 1998;19:1639–62.
 50. Wang J, Lenardo MJ. Roles of caspases in apoptosis, development, and cytokine maturation revealed by homozygous gene deficiencies. *J Cell Sci* 2000;113:753–7.
 51. Lo KK-W, Lee TK-M, Lau JS-Y, et al. Luminescent biological probes derived from ruthenium(II) estradiol polypyridine complexes. *Inorg Chem* 2008;47:200–8.
 52. El-Helby AGA, Ayyad RR, Sakr HM, et al. Design, synthesis, molecular modeling and biological evaluation of novel 2, 3-dihydrophthalazine-1, 4-dione derivatives as potential anti-convulsant agents. *J. Mol Struct* 2017;1130:333–51.
 53. Al-Warhi T, Abo-Ashour MF, Almahli H, et al. Novel [(N-alkyl-3-indolylmethylene)hydrazono]oxindoles arrest cell cycle and induce cell apoptosis by inhibiting CDK2 and Bcl-2: synthesis, biological evaluation and in silico studies. *J Enzyme Inhib Med Chem* 2020;35:1300–9.
 54. Eldehna WM, Nocentini A, Elsayed ZM, et al. Benzofuran-based carboxylic acids as carbonic anhydrase inhibitors and antiproliferative agents against breast cancer. *ACS Med Chem Lett* 2020;11:1022–7.
 55. Sabt A, Eldehna WM, Al-Warhi T, et al. Discovery of 3,6-disubstituted pyridazines as a novel class of anticancer agents targeting cyclin-dependent kinase 2: synthesis, biological evaluation and in silico insights. *J Enzyme Inhib Med Chem* 2020;35:1616–30.
 56. Eldehna WM, Hassan GS, Al-Rashood ST, et al. Synthesis and in vitro anticancer activity of certain novel 1-(2-methyl-6-arylpyridin-3-yl)-3-phenylureas as apoptosis-inducing agents. *J Enzyme Inhib Med Chem* 2019;34:322–32.
 57. Alesawy MS, Al-Karmalawy AA, Elkaeed EB, et al. Design and discovery of new 1, 2, 4-triazolo [4, 3-c] quinazolines as potential DNA intercalators and topoisomerase II inhibitors. *Archiv Der Pharmazie* 2020.
 58. El-Zahabi MA, Elbendary ER, Bamanie FH, et al. Design, synthesis, molecular modeling and anti-hyperglycemic evaluation of phthalimide-sulfonylurea hybrids as PPAR γ and SUR agonists. *Bioorg Chem* 2019;91:103115.

59. Ibrahim MK, Eissa IH, Alesawy MS, et al. Design, synthesis, molecular modeling and anti-hyperglycemic evaluation of quinazolin-4(3H)-one derivatives as potential PPAR γ and SUR agonists. *Bioorg Med Chem* 2017;25:4723–44.
60. Ibrahim MK, Eissa IH, Abdallah AE, et al. Design, synthesis, molecular modeling and anti-hyperglycemic evaluation of novel quinoxaline derivatives as potential PPAR γ and SUR agonists. *Bioorg Med Chem* 2017;25:1496–513.
61. El-Gamal KM, El-Morsy AM, Saad AM, et al. Synthesis, docking, QSAR, ADMET and antimicrobial evaluation of new quinoline-3-carbonitrile derivatives as potential DNA-gyrase inhibitors. *J Mol Struct* 2018;1166:15–33.
62. Eissa IH, El-Helby A-GA, Mahdy HA, et al. Discovery of new quinazolin-4(3H)-ones as VEGFR-2 inhibitors: design, synthesis, and anti-proliferative evaluation. *Bioorg Chem* 2020;105:104380.
63. El-Adl K, El-Helby A-GA, Ayyad RR, et al. Design, synthesis, and anti-proliferative evaluation of new quinazolin-4 (3H)-ones as potential VEGFR-2 inhibitors. *Bioorg Med Chem* 2021;29:115872.